

Index

Chapter 1: Introduction	4
Vaccine adjuvants	4
TLRs-dependent adjuvants	6
Examples of TLRs-dependent adjuvants and their mechanisms of action.	10
TLRs-independent adjuvants	12
Alum	12
Mechanism of adjuvanticity	13
MF59 oil-in-water emulsion	15
Mechanism of adjuvanticity	17
Involvement of transendothelial migration in adjuvanticity.	20
Preclinical experience of MF59	24
Clinical experience of MF59	25
Purpose of the project	27
Chapter 2: Materials and Methods	29
Reagents and buffers	29
Adjuvant and antigens	29
Mice	30
Immunization schedule	30
Microarray analysis	32
Muscle RNA extraction and purification	32
Lymph nodes RNA extraction and purification	33
RNA quantification and quality assessment	34
Concentration measurement	34

Quality measurement	34
RNA labelling and purification	35
Microarray hybridization and data acquisition	35
Microarray data analysis	36
FACS analysis of lymph nodes cell preparation	37
Lymph node cell preparation	37
Lymph node cell staining	37
FACS analysis	38
Hemoagglutination inhibition test	38
ELISA test	39
Confocal analysis	40
Muscles	40
Lymph nodes	40
Mouse cytokine assay	41
Chapter 3: Results	44
The activity of different vaccine adjuvants depends on the antigen.	44
MF59 is the strongest activator of gene transcription in the mouse muscle, while R848 activate gene expression in the LNs.	49
R848 induces CD69 and CD86 expression in the LNs on T/NK and B cells respectively.	57
MF59 activates transendothelial migration genes at the injection site.	64
MF59 and Pam3CSK4 activate GL7 expression in the Germinal Centers of the lymph node.	69

Chapter 4: Discussion of results and overview	72
Chapter 5: References	78
Acknowledgements	83

1. Introduction

1.1 Vaccine adjuvants

Adjuvants are helper substances able to strengthen the immune response against antigens when used in combination with vaccines. They have been defined by Janeway as the immunologist's 'dirty little secret', meaning that such substances radically improve the vaccine efficacy through mechanisms that are not yet fully elucidated. The "adjuvant effect" was described for the first time in 1926 [1] when Ramon defined adjuvants as "substances used in combination with a specific antigen that produce more immunity than the antigen alone" [2].

The reasons why adjuvants play a fundamental role in vaccine development are that they increase immunogenicity of weak antigens, as mentioned and they allow to decrease the dose of the antigens in vaccine formulations, to extend the speed and the duration of the immune response by enhancing memory B and T cell responses and to modulate antibody avidity, specificity, isotype or subclass distribution.

Adjuvants work via different mechanisms. They create a depot of antigen at the injection site, resulting in a gradual release of small quantities of antigen over a long period of time. The adjuvant also serves as a vehicle for delivering the antigen to the lymphoid organs, where antigenic epitopes can be presented to T cells by professional antigen-presenting cells (APCs). Furthermore, due to advances in the immunological research of the last decades, adjuvants are known to activate many immune cell types acting on mechanisms of the innate and adaptive immune response. In conventional procedures used for protein and DNA vaccination, adjuvants are co-injected together with the antigen, and they stimulate the immune system by triggering either the innate or the adaptive immunity.

In mammals, the crucial event responsible for the initiation of an adequate immune response is antigen recognition, uptake and presentation to naive lymphocytes by dendritic cells (DCs), the so-called "professional APCs". These DCs, being resident in organs, act as sentinels in the periphery and are specialized in capturing antigens by receptor-mediated endocytosis and pinocytosis mechanisms in order to undergo a complex multistep maturation process. DC

maturation occurs in response to the encounter of the antigen and in presence of microbial and pathogen-derived signals which increase DCs capacity to migrate towards the draining lymph nodes. On their journey to lymphoid organs, DCs interact with several ligands, in particular chemokines which can further enhance the DC maturation process. Once they reach lymph nodes, DCs shift from an antigen-capturing cell to a T-cell sensitising cell. DCs present the antigen in the context of the MHC molecule to T cells and activates T lymphocyte clonal expansion and memory development via expression of co-stimulatory molecules (CD80, CD86 and CD40) and cytokine production [4].

Vaccine adjuvants are commonly divided in two different classes (fig 1.1), depending on their nature and on their mechanism of action: compounds derived from microbial components, agonists of Toll-like receptors (TLRs), are known as TLRs-dependent adjuvants; other compounds, such as mineral salts, microparticles or emulsions are defined as TLRs-independent adjuvants.

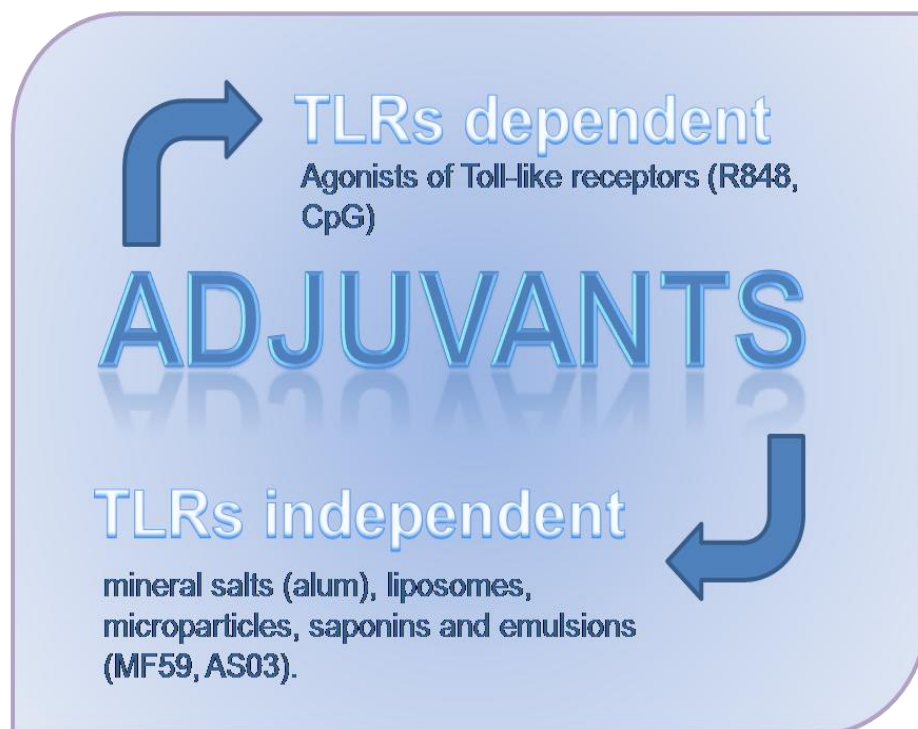


Figure 1.1: Two classes of vaccine adjuvants: TLR-dependent and TLR-independent adjuvants.

1.2 TLRs-dependent adjuvants

Toll-like receptors (TLRs) are the best studied class of pattern recognition receptors (PRRs) of the innate immune system and are expressed on various immune cells, including macrophages, DCs, B cells, specific types of T cells, and even on non-immune cells such as fibroblasts and epithelial cells. Expression of TLRs is not static but rather is modulated rapidly in response to pathogens, a variety of cytokines, and environmental stresses. TLRs may be expressed extra- or intracellularly (fig 1.2). TLRs 1, 2, 4, 5, and 6 are expressed on the cell surface, while TLRs 3, 7, 8, and 9 are found almost exclusively in intracellular compartments such as endosomes, and their ligands, mainly nucleic acids, require internalization to the endosome before signaling is possible. [3] Cell surface TLR1, TLR2, and TLR6 recognize lipoproteins, TLR4 recognizes lipopolysaccharide (LPS), and TLR5 (or TLR11, which is not functional in humans) recognizes a pathogen-derived protein, flagellin. The endosomal TLR3 and TLR7, TLR8, and TLR9 recognize nucleic acids as unmethylated CpG motifs, double and single strand RNA poly(I:C) [6].

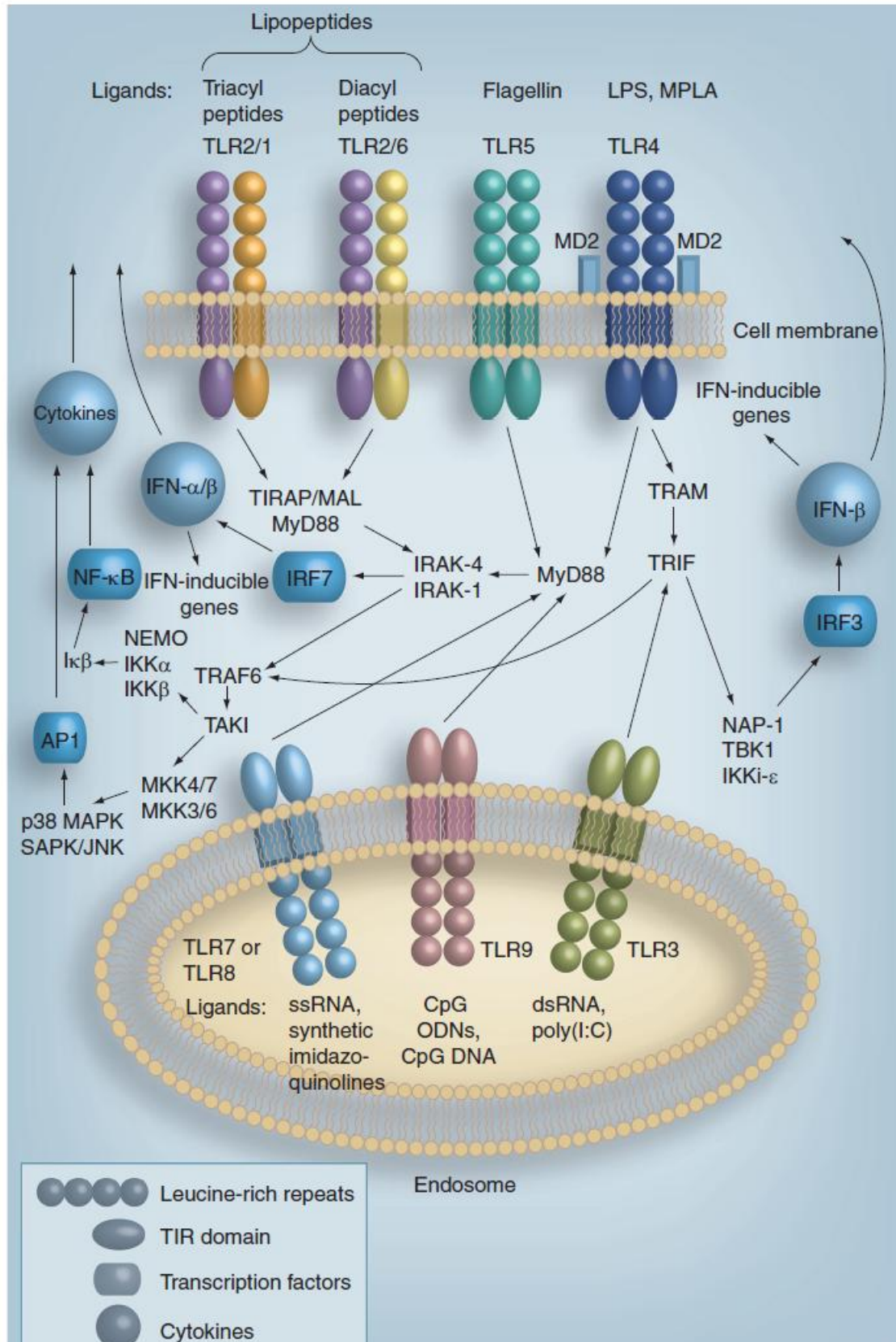


Figure 1.2: Cellular distribution of TLRs and their signaling pathway: (taken from Black M *et al* Advances in the design and delivery of peptide subunit vaccines with a focus on Toll-like receptor agonists, 2010). TLRs 1, 2, 4, 5, and 6 are expressed on the cell surface, others (TLRs 3, 7, 8, and 9) are found almost exclusively in intracellular compartments such as endosomes. The TLRs initiate complex intracellular signaling pathways, resulting in the production of various cytokines that dictate specific immune responses. Typical ligands for the TLR domains are shown. AP1: Activator protein 1; IFN: Interferon; IKK: I κ Ba kinase complex; IRAK: IL-1 receptor-associated kinase; IRF: Interferon regulatory factor; MAL/TIRAP: MyD88 adapter-like TIR domain-containing adapter protein; MAPK: Mitogen-activated protein kinase; MKK: Mitogen-activated protein kinase kinase; MyD88: Myeloid differentiation primary-response gene 88; NAP: NF- κ B-activating kinase-associated protein; NEMO: NF- κ B essential modulator; ODN: Oligodinucleotide; SAPK/JNK: stress-activated protein kinase/c-Jun NH2-terminal kinase; TAK: Transforming growth factor- β -activated kinase; TBK: TANK-binding kinase; TIR: Toll/IL-1 receptor; TLR: Toll-like receptor; TRAF: TNF receptor-associated factor; TRAM: TRIF-related adapter molecule; TRIF: TIR-domain-containing adapter inducing IFN- β .

This class of adjuvants are pathogen-associated molecular patterns (PAMPs) and can activate TLRs on the surface of dendritic cells (DCs) and other cell types [3,4].

The direct stimulation of DCs leads to initiation of Th cell response that requires events show in the figure 1.3. The first signal (signal 0), is based on the stimulation of pattern recognition receptors on macrophages and DCs by pathogen-associated molecular patterns (PAMPs). As a result of this activation, DCs mature and are licensed to present antigens. The lymphocyte T-cell receptor (TCR) sensitization takes place following interaction with the MHC – peptide complex (signal 1). This is followed by T-cell activation against the antigen via co-stimulatory molecules interaction (signal 2), and by a cytokine expression pattern that orientates T-cell differentiation towards the TH1 or TH2 specific functional pathway (signal 3). [5].

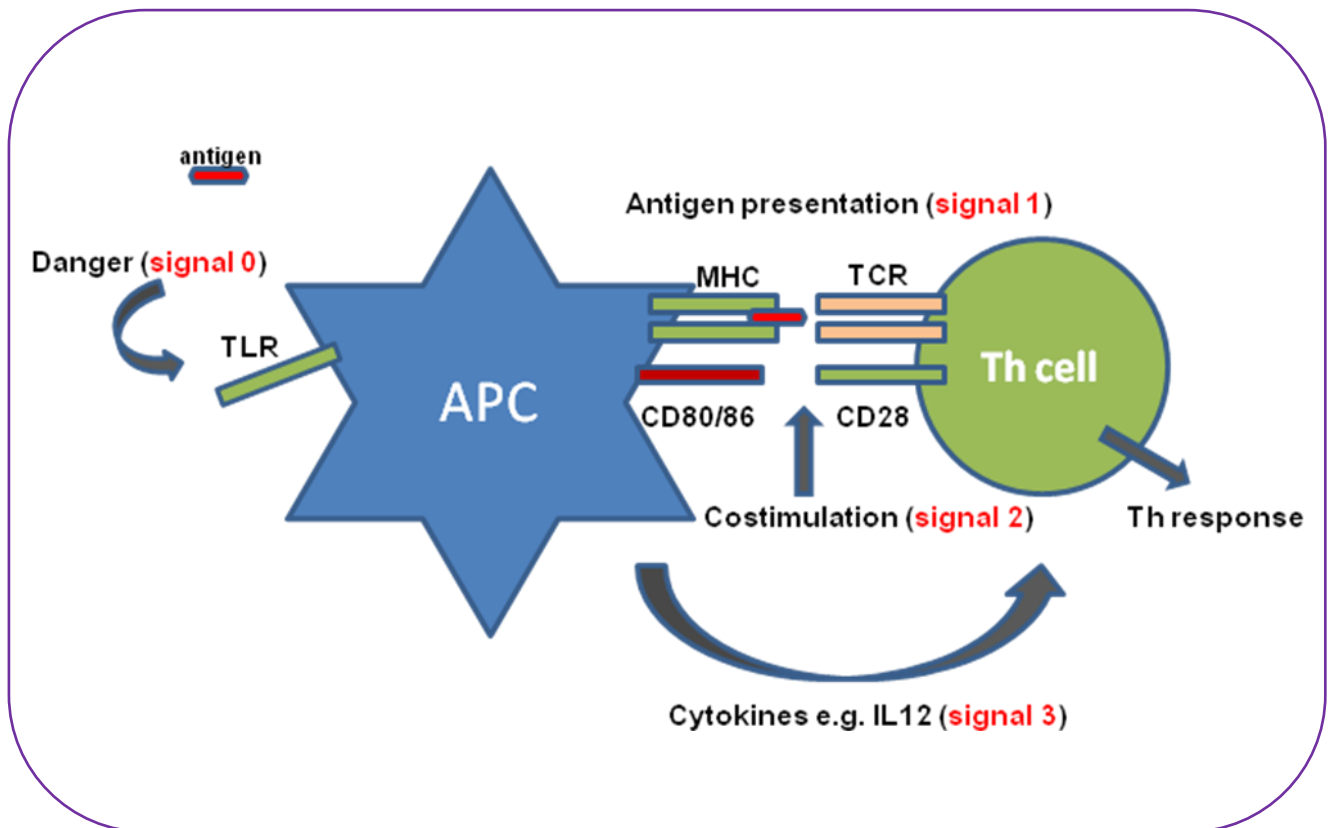


Figure 1.3: Stimulation of TLRs: The first signal (signal 0) is represented by the stimulation of TLRs, expressed on APCs. These cells are activated by pathogen-associated molecular patterns (PAMPs) as the antigen. Then DCs mature and are licensed to present antigens. The lymphocyte T-cell receptor (TCR) sensitization takes place following interaction with the MHC–peptide complex (signal 1). It is followed by T-cell activation against the antigen via co-stimulatory molecules interaction (signal 2), and by a cytokine expression pattern that orientates T-cell response (signal 3).

1.2.1 Examples of TLRs-dependent adjuvants and their mechanisms of action.

The most widely studied TLR ligand is LPS. LPS is a Gram-negative membrane molecule consisting of a hydrophilic polysaccharide and a lipophilic phospholipid (lipid A). The lipophilic portion of LPS is such a potent stimulus on the pro-inflammatory cytokine production that it can lead to septic shock whereas monophosphoryl lipid A (MPL) is a lipid A derivative included in many adjuvant formulations because it retains good adjuvanticity and lower toxicity. The adjuvanticity of these molecules depends on their capability to bind and activate the TLR4.

CpG-DNA is an immunostimulatory oligodeoxynucleotide, consisting of unmethylated CpG motifs which are recognized by TLR9, so leading to activation of innate immunity and cytokine-dependent promotion of the Th1 response. These motifs, present in bacterial DNA, consist of an unmethylated CpG dinucleotide flanked by two 5' purines and two 3' pyrimidine. During an infection, the release of unmethylated CpG-DNA from bacteria serves as a danger signal that stimulates the immune system of the host. Bacterial DNA and synthetic unmethylated CpG oligodeoxynucleotides trigger an immunostimulatory cascade that culminates in maturation, differentiation and proliferation of several immune cells creating a pro-inflammatory and Th1-biased environment. Addition of the immunostimulatory CpG-DNA to peptide vaccines, shifts the balance towards a Th1 immune response, which is often accompanied by a significant increase in IgG2a production [45].

Imidazoquinoline molecules, including imiquimod and resiquimod (R848), are selective TLR7 and TLR7/8 agonists, respectively [50]. As mentioned before, TLR7 and 8 are expressed intracellularly in endocytic vesicles and endosomal acidification is important for activation by imiquimod and resiquimod, because agents that block endosomal acidification inhibit immune activation by these agents [52]. Upon activation through TLR7 and 8, a cascade of signaling events occur that initiate through myeloid differentiation primary response gene (MyD88), IL-1 receptor-activated kinase (IRAK) and TNF receptor-activated factor-6 (TRAF6) [51]. This eventually leads to activation of a number of transcription factors including NF- κ B (fig 1.2) and IFN regulatory factors (IRF) including IRF-5 and IRF-7. IRF-5 appears to be required for NF- κ B induction and proinflammatory cytokine production by TLR7 agonists, whereas IRF-7 is required for IFN- α production. In addition to stimulating

cytokine production from DCs, imiquimod and resiquimod lead to maturation of DC subpopulations: they stimulate pDCs to express the costimulatory molecules CD40, CD80 and CD86 as well as increasing the expression of chemokine receptor CCR7, important for homing of DCs to T-cell zones. Moreover this class of toll-agonists polyclonally activate B cells to proliferate and differentiate into antibody-secreting cells and can, in some cases, induce class switching [52].

Among the TLR2 ligands, lipoproteins and lipopeptides are the major components of the outer membrane of bacteria and anchored onto the membrane. In particular the cell wall of Gram-positive bacteria contains a thick layer of peptidoglycan (PGN) within which lipoproteins and lipoteichoic acids are embedded. Analysis of TLR2-deficient mice demonstrated clearly that TLR2 is essential for the response to PGN [54]. One of the Mycoplasma lipopeptides, the 2 kDa macrophage-activating lipopeptide-2 (MALP-2), was shown to utilize TLR2 as its signal transducer [55]. It has been demonstrated that TLR2 forms heterodimers with other TLRs (TLR1 and TLR6): coexpression of TLR2 with TLR6 could confer NF- κ B activation and cytokine production, while cells expressing TLR2 alone could not [56]. Pam3CSK4 is a synthetic tripalmitoylated lipopeptide that mimics bacterial lipopeptides: it has been shown that it can activate the proinflammatory transcription factor, NF- κ B, in a TLR2- dependent manner [57].

Many other adjuvants are water-in-oil formulations containing PAMPs of microbial derivation. Freund's complete and incomplete adjuvant is recognised as being as one of the most effective water-in-oil adjuvant. The complete formulation (FCA) has been developed as a water-in-oil emulsion containing heat-killed Mycobacteria. The potent effect of FCA on the immune response is due to the ability of inactivated bacteria to stimulate TLRs, although the adverse effects on the host caused by Mycobacteria have discouraged scientists from using Freund's in clinical trials [45].

\

1.3 TLRs-independent adjuvants

The class of TLRs-independent adjuvants include mineral salts, liposomes, microparticles, saponins and emulsions. These are particulate compounds and are generally defined antigen delivery systems.

These adjuvants interact with APCs and antigens in an unspecific manner, increasing antigen persistency. They indirectly stimulate APCs through activation of other blood cells or structural cells, that induce the production of cytokines which generate a local immunostimulatory environment; they can also activate innate immune pathway such as the NOD-like receptor 3-dependent pathway NALP3 and induce differentiation of monocytes into mature DCs.

It has been proposed that particulate adjuvants should be combined to TLR agonists to optimize vaccines based on soluble and otherwise poorly immunogenic proteins [7]. In fact it is important mentioning that MPL, the only TLR-dependent adjuvant approved for human use, is adsorbed to alum mineral salts together with the target antigens from HBV or HPV viruses in the licensed vaccines [8].

1.3.1 Alum

Aluminum-containing adjuvants have been in use for more than 80 years and continue to be the most widely used clinical adjuvants. Alum is water-soluble aluminum potassium sulfate $AlK(SO_4)_2$ to which a solution of antigen in phosphate buffer is added, followed by precipitation through addition of a basic solution such as NaOH: the precipitate is chemically amorphous aluminum hydroxyphosphate.

The adjuvants that are licensed for use in humans are aluminum hydroxide ($Al(OH)_3$) and aluminum phosphate (chemically amorphous $Al(OH)_x(PO_4)_y$ in which some hydroxyl groups of $Al(OH)_3$ are replaced by a phosphate group, and whose precise composition depends on the method of preparation) [9].

1.3.1.1 Mechanism of adjuvanticity

Despite that alum have been used since a long time, the reasons of the its adjuvanticity is still not completely clear. Probably the immuno-modulating and immuno-stimulating effects of aluminium compounds result from several mechanisms of action.

The first described effect was called “depot effect” as a result of the absorption of the antigen. The major forces for this absorption are electrostatic and hydrophobic attractions and ligand exchanges: these cause a delayed clearing of the complexed antigen from the injection site by building a depot, from which the antigen is released very slowly [10]. Several published studies however demonstrate that adsorption to alum does not increase significantly antigen half life *in vivo* [11-13].

Secondly, alum leads the induction of local proinflammatory reactions at the site of injection, it stimulates DCs. Alum-dependent increase of antigen uptake by DCs was shown *in vitro* [14]. Moreover the involvement of these antigen presenting cells in alum adjuvanticity was proved by the fact that, conditionally depleting CD11c+ monocytes or DCs, the effect of alum in cellular and humoral immunity is abolished [15]. It has been also proposed that aluminium-containing adjuvants can induce DCs mobilization and maturation [14]. Kool M. et al. demonstrated that, *in vivo*, following i.p. injection, alum leads to an attraction of neutrophils, eosinophils, and particularly inflammatory Ly6C+/CD11b+ monocytes, into the peritoneal cavity, driven by an acute production of IL-8, CCL11 and CCL2 (fig. 1.4). Monocytes consequently take up antigen and migrate to the draining lymph nodes where they become monocyte-derived DCs that express high levels of MHC class II and CD86 [15].

Several papers have shown that the combination of alum with TLR-dependent adjuvant, such as CpG or LPS, leads to an enhancement of humoral and cellular responses with respect to alum or the other adjuvants alone [16]. Even though experiments performed in MyD88-TRIF double mutant mice have demonstrated that alum adjuvanticity is independent of functional TLR pathways [17], suggesting another pathway linked to this effect.

Indeed, different *in vitro* and *in vivo* studies suggest the involvement of NALP3, the most studied NOD-like receptors (NLRs) family member, in the adjuvant effect induced by alum. NALP3 is a cytoplasmic receptor which associate with ASC and the caspase 1 protease to form a protein complex called the NLRP3 inflammasome [18]. This complex is activated by multiple agonists, including bacterially derived MDP or endogenous ATP and uric acid and

this activation leads to the cleavage and release of important proinflammatory cytokines such as IL-1b, IL-18, and IL-33 [19]. Since it has been demonstrated a caspase-1-dependent production of IL-1b and IL-18 in human DCs and macrophages following stimulation with a combination of TLR4 agonist and alum [20], several groups have performed experiments on alum adjuvanticity using mice deficient in different NALP3 inflammasome subunits. Macrophages and DCs from mice deficient in NALP3 or ASC had impaired production of IL-1b following alum/LPS exposure *in vitro* and reduced IL-1b production *in vivo* following i.p. injection of alum [21-24], suggesting that the direct activation of NALP3 has a role in alum adjuvanticity. It has been proposed another mechanism for NALP3 activation that involves the production of uric acid, an activator of Nalp3 [25]. Injection of alum would lead to cell necrosis with release of uric acid from macrophages and neutrophils that activate NALP3. In addition to being a sign of necrotic cell death, uric acid is also produced in response to oxidative stress induced by aluminum-containing adjuvants, as it is one of the best endogenous antioxidant molecules that particularly react with hydroxyl radicals [26]. The innate cytokines, such as IL1b, can increase transcription of xanthine oxidoreductase, the enzyme responsible for the formation of uric acid from xanthine [27]. However the precise cellular source of uric acid that is induced by alum injection still needs to be elucidated and this mechanism of action needs further investigation.

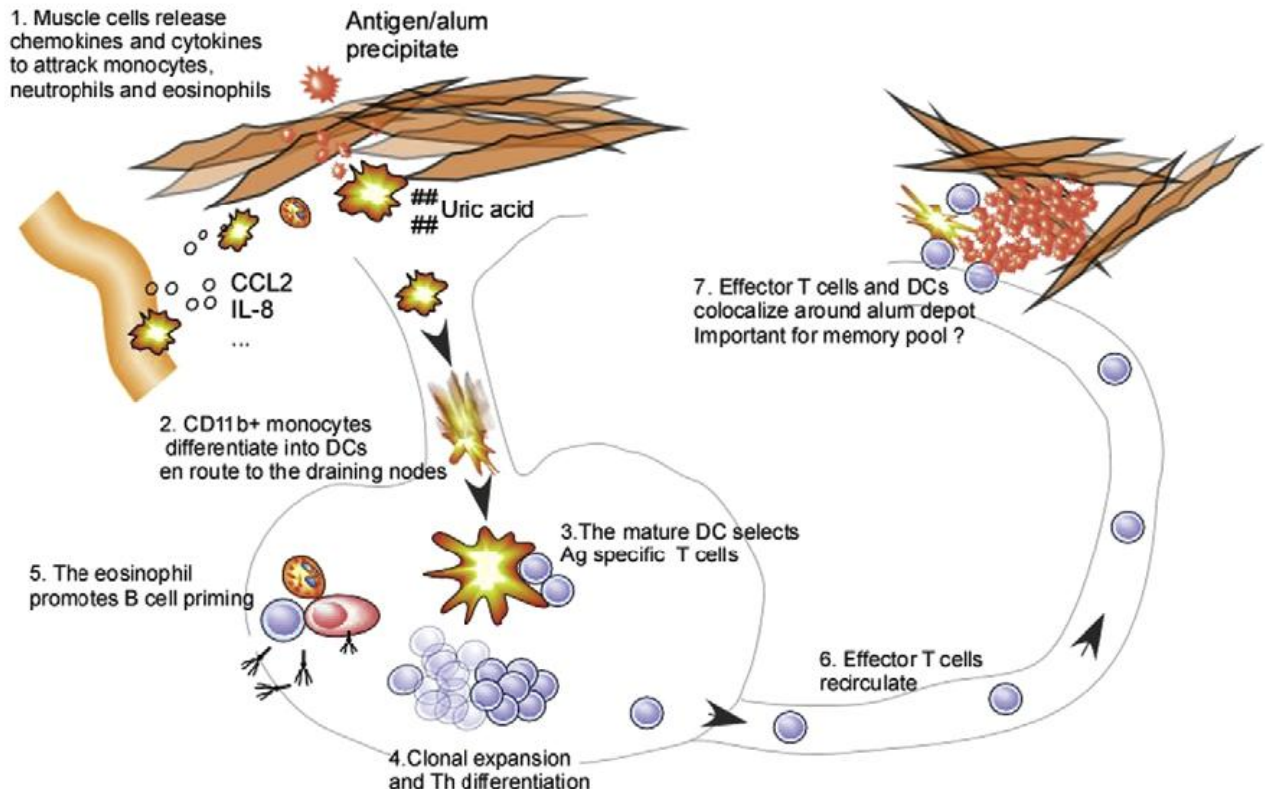


Figure 1.4 (taken from Lambrecht B N *et al.*, Current Opinion in Immunology 2009) **Overview of immune response induced by alum adjuvant**

1.3.2 MF59 oil-in water emulsion

Together with alum, the most widely used adjuvant, the European Medicinal Evaluation Agency has licensed for human use three other adjuvants in the last ten years: the oil-in-water emulsions MF59 and AS03 and the TLR4-agonist monophosphoryl lipid A formulated in alum (AS04) [28].

MF59 is a squalene-based oil-in-water emulsion consisting of small (~160 nm in diameter), uniform, and stable microvesicles, consisting of a drop of oil surrounded by a monolayer of non-ionic detergents (figure 1.5).

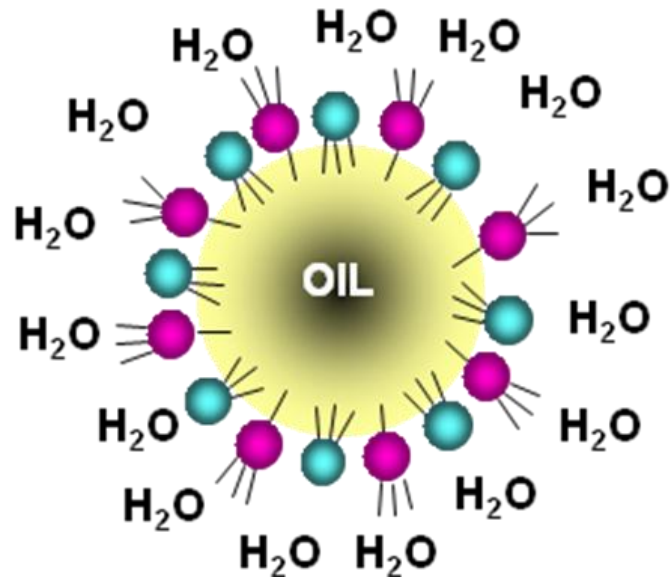


Figure 1.5 Schematic representation of the MF59 oil-in-water emulsion

The oil is squalene, obtained from shark liver. Squalene is a natural component of cell membranes, is found in human sebum (a skin surface lipid) and is a naturally occurring hydrocarbon precursor of cholesterol. Squalene droplets are stabilized by addition of two non-ionic surfactants, a low hydrophilic–lipophilic balance (HLB) surfactant, Polysorbate 80 (Tween 80), and sorbitan triolate (Span 85) (see table 1.1) [29].

Composition of MF59	
Appearance	Milky white oil-in-water emulsion
Composition	0.5% Tween 80 0.5% Span 85 4.3% Squalene Water for injection 10 nM Na-Citrate buffer
Density	0.9963 g/ml
Viscosity	Close to water
Size	160 ± 10 nm

Table 1.1 Composition of MF59 oil-in-water emulsion

MF59 was initially developed by Chiron Vaccines as vehicle for muramyl peptide adjuvant MTP-PE, a synthetic version of MDP, a molecule identified as natural component of mycobacterial cell wall. Several experiments showed that MF59, even in the absence of the immune potentiator, had adjuvant properties itself, encouraged moving the development of MF59 as a standalone adjuvant for flu vaccines [30]

1.3.3.1 Mechanism of adjuvanticity

A wide variety of vaccine antigens has been formulated with MF59. The adjuvant activity of MF59 display very different physico-chemical characteristics indicate the versatility of this adjuvant. These antigens range from monomeric (HIV gp120) to particulate (surface antigens from hepatitis B virus), and from soluble (HSV-2 gD2) to insoluble (influenza virus haemagglutinin) antigens [29]. An influenza adjuvanted vaccine (Fluad) was developed by combining MF59 with the two main influenza antigens HA and NA and was in use in more

than 20 countries over the last decade. Despite that, the precise mechanism of action of MF59 adjuvanticity remains still unclear.

Studies conducted with fluorescently-labelled MF59 have shown that MF59 does not have a “depot effect”: 4 h after intramuscular administration, 36% of injected adjuvant was still present in the muscle and the peak of localization in the corresponding lymph nodes was reached 2 days after injection. Moreover the presence of adjuvant did not influence the distribution of the co-administered antigen (HSV-2 gD2), which was cleared from the site of injection independently of MF59. Two days after intramuscular injection, MF59 localized in the draining lymph node and was shown to be partially located in T-cell areas within lymph node-resident cells that had the characteristics of antigen-presenting cells (fig.1.6). This observation suggested that MF59 can induce infiltration in the muscle and then activation of monocytes that take up the antigen and transport it to the nodes where they differentiate into DCs. Indeed, immunofluorescence analysis demonstrated that administration of MF59 promoted antigen uptake by DCs and also induced a significant influx of macrophages at the site of injection, which was significantly suppressed in mice deficient for chemokines receptor 2 (CCR2) [31,32].

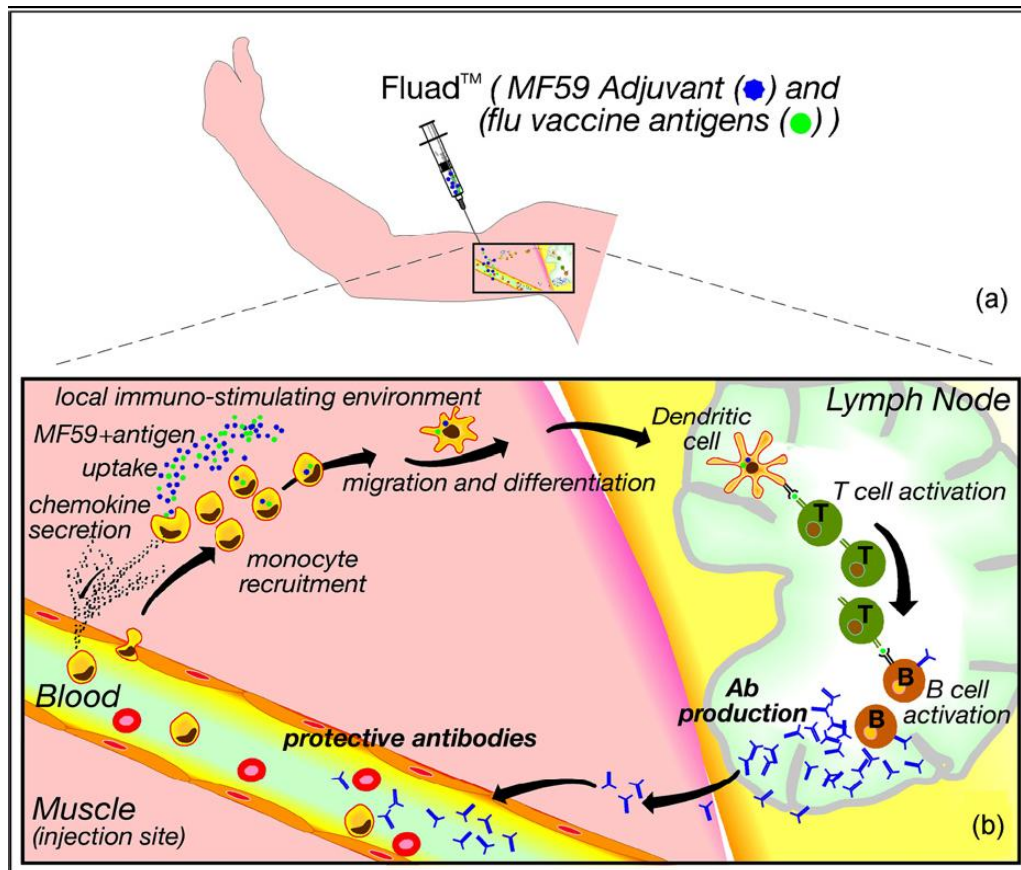


Fig. 1.6 MF59 uptake, monocyte recruitment, migration, T-/B-cell activation and differentiation (taken from Schultze V, *et al.* Safety of MF59 adjuvant. Vaccine 2008.

Mosca *et al.*, in agreement with previous mentioned data, using genome wide microarray analysis, demonstrated that MF59 similarly to alum and CpG, leads the activation of innate immune reactions after i.m. injection in mice. They shown that all adjuvants activate a core set of genes named “adjuvant core response genes” including cytokines (Il-1b, Il-2), chemokines (Ccl2, Ccl4, Ccl5, Ccl12, Ccl10) and adhesion molecules, suggesting that the establishment of a local immunocompetent environment associated to a nonpathogenic inflammatory process is generally associated to vaccine adjuvanticity. Interestingly they observed that, in the muscle, MF59 was more potent in inducing upregulation of immune-related genes than alum and CpG. MF59 also induced the up-regulation of genes coding for Ccr2 and its ligands (Ccl2, Ccl7 and Ccl8) supporting previous data showing that cell recruitment at injection site is driven by CCR2. Furthermore, the same study showed that MF59 promoted a more rapid influx of CD11b+ cells in the muscle compared to other

adjuvants. Some of the early genes up-regulated by MF59 were used as biomarkers to identify MF59 target cells. Confocal analysis demonstrate that two of these biomarkers, JunB and Pentraxin 3, were up-regulated in muscle fibers following MF59 treatment, suggesting that muscle cells are a target of MF59 *in vivo* [33].

1.3.3.2 Involvement of transendothelial migration in adjuvanticity

As described before, transendothelial migration events are an important mechanism of adjuvanticity, in particular if we are talking about the oil in water emulsion MF59.

The recruitment of activated phagocytes to sites of infection occurs as part of the inflammatory response and is mediated by cell-adhesion molecules that are induced on the surface of local blood vessel endothelium. Several structural families of adhesion molecules have a role in leukocyte migration, homing and cell-cell interaction: the selectins, the integrins and protein of the immunoglobulin superfamily (see table 1.2). The table shows an example from each family, a list of other family members that participate in leukocyte interactions, their cellular distribution and their ligand in adhesive interactions [44].




		Name	Tissue distribution	Ligand
Selectins		P-selectin (PADGEM, CD62P)	Activated endothelium and platelets	PSGL-1, sialyl-Lewis ^x
		E-selectin (ELAM-1, CD62E)	Activated endothelium	Sialyl-Lewis ^x
Integrins		$\alpha_L:\beta_2$ (LFA-1, CD11a:CD18)	Monocytes, T cells, macrophages, neutrophils, dendritic cells	ICAMs
		$\alpha_M:\beta_2$ (CR3, Mac-1, CD11b:CD18)	Neutrophils, monocytes, macrophages	ICAM-1, iC3b, fibrinogen
		$\alpha_X:\beta_1$ (CR4, p150.95, CD11c:CD18)	Dendritic cells, macrophages, neutrophils	iC3b
		$\alpha_5:\beta_1$ (VLA-5, CD49d:CD29)	Monocytes, macrophages	Fibronectin
Immunoglobulin superfamily		ICAM-1 (CD54)	Activated endothelium	LFA-1, Mac1
		ICAM-2 (CD102)	Resting endothelium, dendritic cells	LFA-1
		VCAM-1 (CD106)	Activated endothelium	VLA-4
		PECAM (CD31)	Activated leukocytes, endothelial cell-cell junctions	CD31

Table 1.2 (taken from Janeway's Immunobiology, Seventh edition): classes of adhesion molecules involved in leukocyte interaction.

The selectins are membrane glycoproteins that binds specific carbohydrates groups: members of this family are induced on activated endothelium and initiate endothelium-leukocyte interactions by binding to fucosylated oligosaccharide ligands on passing leucocytes. The next step in leukocytes recruitment depends on tighter adhesion, which is due to the binding of intercellular adhesion molecules (ICAMs) on the endothelium to heterodimeric proteins of the integrin family of leukocytes. The leucocyte integrins important for extravasation are LFA-1 ($\alpha_L:\beta_2$, also known as CD11a) and CR3 ($\alpha_M:\beta_2$, complement receptor type 3 also known as CD11b or Mac-1/Itgam) and they both bind to ICAM-1 and ICAM-2 (see fig. 1.7). Strong

adhesion between leukocytes and endothelial cells is promoted by the induction of ICAM-1 on inflamed endothelium and the activation of a conformational change in LFA-1/CD11a and CR3/CD11b/Itgam, that occurs in response to chemokine binding by the leukocytes [44].

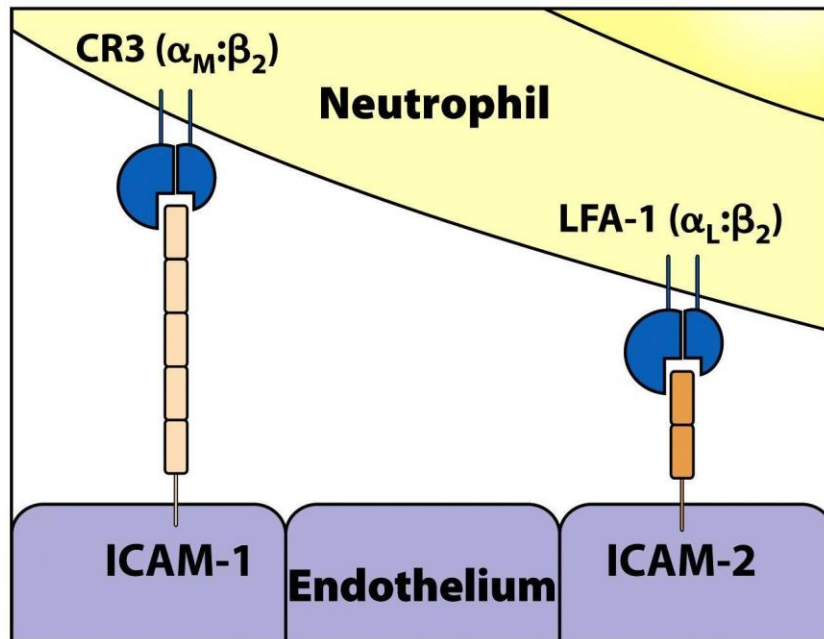


Figure 1.7 (taken from Janeway's Immunobiology, Seventh edition): Phagocyte adhesion to vascular endothelium is mediated by integrins.

The first step of neutrophils migration involves the reversible binding of a neutrophil to vascular endothelium through interaction between selectins (on the endothelial cell) and their carbohydrate ligands (shown in the fig. 1.7). This interaction cannot anchor the cells against the force of the blood flow and they roll along the endothelium, continually making and breaking contacts. The interaction becomes stronger when binding of a chemokine such as CXCL8 to its specific receptor on the neutrophil trigger the activation of the integrins LFA-1/CD11a and CR3/CD11b/Itgam. Inflammatory cytokines such as TNF-α are also necessary to induce the expression of adhesion molecules such as ICAM-1 and ICAM-2, the ligands for LFA1 and CR3, on the vascular endothelium. Tight binding between ICAM-1 and the integrins arrests the rolling and allows the neutrophil to squeeze between the endothelial cells forming the wall of the blood vessel and then to extravasate. The neutrophil also needs to

traverse the basement membrane: it penetrates this with the aid of matrix metalloproteinase enzymes (MMPs) that are expressed at the cell surface. Finally, the neutrophil migrates along concentration gradient of chemokines (shown in the figure 1.8) such as CXCL8, secreted by cells at the site of infection or inflammation [44].

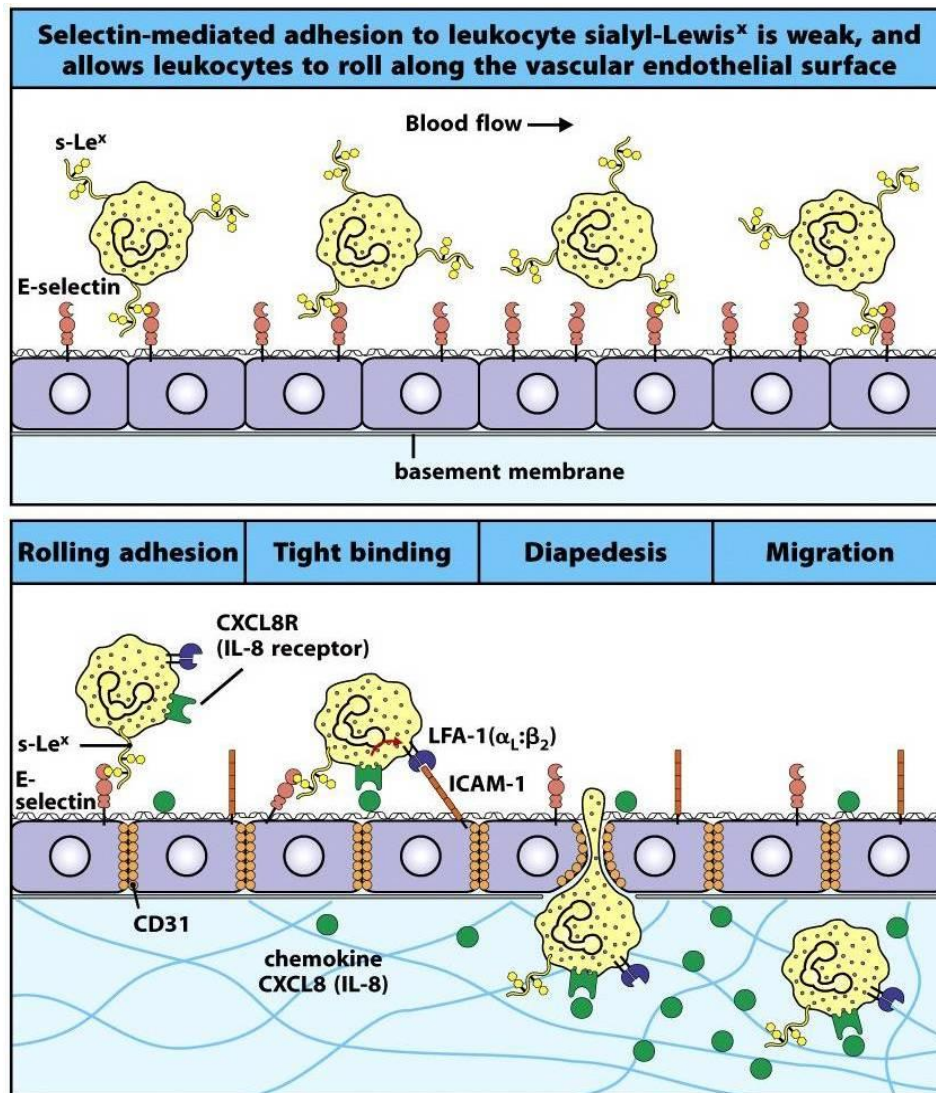


Figure 1.8 (taken from Janeway's Immunobiology, Seventh edition): Neutrophils leave the blood and migrate to sites of infection in a multi-step process.

1.3.3.3 Preclinical experience of MF59

The nonclinical testing of MF59 consist of research studies performed to explore its mechanism of adjuvanticity and also its ability to enhance protection in challenge models. MF59 administered alone or in combination with various antigens, as mentioned before, has been tested in several animal models including mice, rats, Guinea pigs, rabbits, goats, dogs and several non-human primates including chimpanzee [29].

In one of these studies, Wack *et al.*, demonstrated that MF59, in the mouse model, was the most potent adjuvant and induced significantly enhanced HI titers to all seasonal influenza antigens tested (H3N2, H1N1 and B) after one or two doses vaccination (figure 1.9). Moreover for H3N2 can be observed that MF59 induced a substantial increase in HI titers after the second dose, compared to post-1 dose [34].

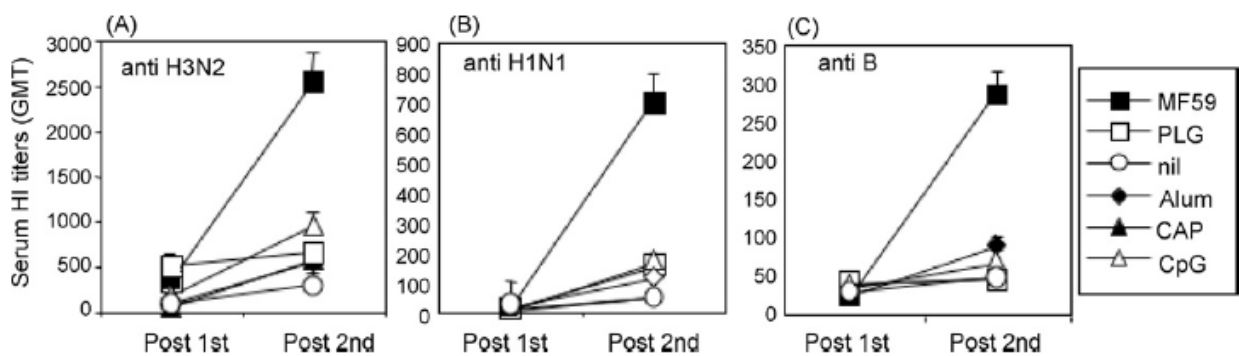


Fig. 1.9 Enhanced HI antibody responses to adjuvanted influenza vaccine. (taken from Wack *et al.*, Combination adjuvants for the induction of potent, long-lasting antibody and T-cell responses to influenza vaccine in mice. Vaccine 2008)

This study compare MF59 with a wide range of different classes of adjuvants, including Alum, calcium phosphate (CAP), a new generation of delivery system such as poly-lactide co-glycolipide (PLG) microparticles and the immune potentiator CpG, which directly activates innate immunity through TLR9 [35]. A significant potency of MF59 was observed in these studies, in comparison to the other tested adjuvants, including Alum. These data are

in line with previous studies on a range of alternative antigens [36, 37] and has important implications for the development of optimal flu vaccines against inter-pandemic strains and in preparations for an influenza pandemic [34].

1.3.3.4 Clinical experience of MF59

Extensive clinical immunogenicity and safety data on various MF59-adjuvanted vaccine antigens have been generated in clinical trials over the last 15 years. The data show that MF59 adjuvanted antigens elicit a strong antibody response, and are safe and generally well tolerated [38]. The clinical findings are significant in the understanding of the adjuvanticity of MF59, and more importantly of the safety of this compound [29].

For example Bernstein *et al.*, conducted a multicenter randomized double-blind study in 394 healthy adults in which they receive 2 intramuscular doses of either saline placebo, influenza A/Vietnam/1203/2004 (H5N1) vaccine alone at different doses, vaccine in combination with MF59, or vaccine at different doses with aluminum hydroxide: blood samples were obtained to determine antibody responses. They found, as shown in figure 1.10, that, 28 days post second immunization, the administration of 15 µg of vaccine in combination with MF59 induce higher hemagglutination-inhibition (HI) and also an higher MN (microneutralization) titers compared to the administration of 30 µg of vaccine in combination with alum or 45 µg of vaccine alone.

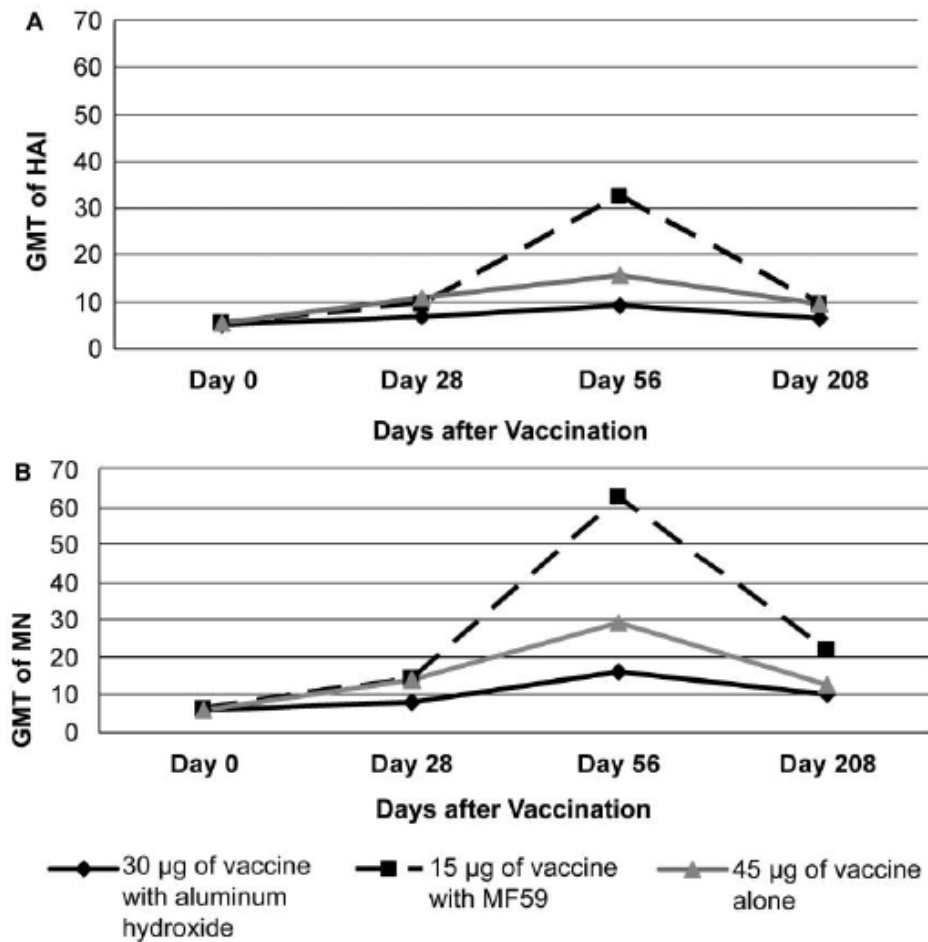


Figure 1.10 Antibody responses over time. (taken from Bernestein *et al.*, Effects of Adjuvants on the Safety and Immunogenicity of an Avian Influenza H5N1 Vaccine in Adults, 2008)

The increased antibody response observed in this study is consistent with previous reports that demonstrate increased antibody titers following vaccination with other A/H5N3 and A/H9N2 avian influenza vaccine [40, 41] or seasonal influenza vaccines [42, 43].

1.4 Purpose of the project

Vaccine adjuvants activate specific innate immune pathways which boost the adaptive response to co-administered antigens. Experimental data in mouse and human, demonstrate that the real efficacy of vaccine adjuvants hinge, in many cases, on the antigen, it's, in other words, antigen-dependent.

The classical example is alum. In human vaccines different form of Alum, aluminium hydroxide, aluminium phosphate and aluminium sulfate, are used. The choice of the formulation depends on how well it adsorbs the protein [58]. Alum has been used for years as an efficient adjuvant for several subunit vaccines such as Hepatitis B and Diphteria-Tetanus. However alum is not very efficient in enhancing the response to flu antigens, as Wack *et al.* demonstrated in their work [16].

On the other hand several works demonstrated that the oil-in-water emulsions, such as MF59, are superior in inducing a good response to flu subunit vaccines. Indeed, in an extensive set of preclinical and clinical studies, the oil-in-water-emulsion MF59 has been found to be a safe and potent vaccine adjuvant, resulting in the licensure of an MF59-adjuvanted influenza vaccine in more than 20 countries. In addition, the highly promising clinical data generated using an influenza pandemic vaccine adjuvanted with MF59 have shown that this adjuvant represents an attractive option for the development of an effective vaccine against a potential pandemic influenza [29].

However, the mechanism of action of flu adjuvanticity, and also the mechanism of action of MF59, is not fully understood.

For these reasons we decided to investigate the innate immune reactions that could be associated to adjuvanticity to flu subunit vaccines *in vitro* and *in vivo* in the mouse system, comparing the effect of MF59 with other classes of adjuvants, including alum and three TLR-dependent adjuvants: the oligonucleotide CpG (TLR9 agonist), the small molecule resiquimod (TLR7/8 agonist) and the lipopeptide Pam3CSK4 (TLR2 agonist).

First we analyzed adaptive response to flu antigens, TT antigens and OVA antigen in combination with MF59 and the other adjuvants listed. Then we performed microarray analysis with the same set of adjuvants (both *in vitro* in mouse splenocytes and *in vivo* in mouse muscle and draining lymph nodes), in order to correlate innate immune gene signatures

induced by the vaccine adjuvants with the ability to boost flu adaptive responses. We validated the activation of some biomarkers in the lymph nodes using FACS analysis and finally we investigated cell recruitment events at the injection site associated with adjuvant administration, performing immunofluorescence analysis of muscle cryosections. Using confocal microscopy, we further analyzed germinal centers formation in the LNs, in order to understand if there is a differential LN structure re-modeling induced by the different adjuvants.

2. Materials and Methods

2.1 Reagents and Buffers

2.1.1 Adjuvants and antigens

The adjuvants used in this study are MF59, alum, CpG, R848 and Pam3CSK4.

MF59 is the Novartis proprietary oil-in-water emulsion adjuvant. It is a microfluidized emulsion consisting of the oil squalene (4.3% w/v) with the two surfactants Tween 80 (polyoxyethylene sorbitan monooleate; 0.85% w/v) and Span-85 (sorbitan trioleate; 0.5% w/v) in a sodium citrate buffer (10 nM). It was stored at 4 °C. Upon use, it was vortexed and used diluted 1:1 in PBS.

The alum used in this study is aluminium hydroxide (Al-OH₃) at 15.03 µg/ml, stored at 4°C.

The CpG used was the 1826 phosphorothioate oligodeoxynucleotide. The sequence is 5'-TCC ATG ACG TTC CTG ACG TT-3'. The lyophilized CpG was re-suspended at 1 mg/ml in MilliQ water, aliquoted and stored at -80°C. When needed, an aliquot was thawed and stored at 4°C for up to one month.

R848 (resiquimod) is an imidazoquinoline acting as a TLR7/8 agonist. The lyophilized R848 was resuspended at 100 mM in 100 % DMSO and stored at -20 °C.

Pam3CSK4 (Invivogen) is synthetic triacylated lipoprotein, agonist of TLR2. The lyophilized Pam3CSK4 was resuspended at 1 mg/ml in MilliQ water, aliquoted and stored at -20°C. When needed an aliquot was thawed and stored at 4 °C up to one month.

The antigens used in this study are trivalent flu antigens from the seasonal flu vaccine formulation, ovalbumin and tetanus toxoid.

The flu antigens were the 2007/2008 seasonal flu antigens. H1N1 (A/Brisbane/59/2007 (H1N1)-like virus), H3N2 (A/Brisbane/10/2007 (H3N2)-like virus), B (B/Florida/4/2006-like virus). They were stored at 4 °C in PBS.

Tetanus toxoid antigen was stored in PBS.

OVA (Hyglos GmbH): EndoGrade Ovalbumin 98% pure, prepared by ion exchange from egg white. The lyophilized OVA was reconstituted in buffer at 1mg/ml, aliquoted and then stored at -20 °C.

2.2 Mice

For all the adjuvanticity, microarray, flow cytometry and confocal microscopy experiments BALB/c mice were used.

All animals were housed and treated according to internal animal ethical committee and institutional guideline.

2.3 Immunization schedule

For all experiments mice were anesthetized with 1ml Ketavet + 0.13 ml Xilro in 10 ml PBS intraperitoneally with 0.01 ml/g of animal weight (corresponding to 50 mg/kg ketamine + 2.6 mg/kg xilazine) and then were immunized intramuscularly in both quadriceps with 50 µl dose/quadricept.

2.3.1 Immunization for adjuvanticity experiments

For adjuvanticity experiments 8 mice/group were injected with trivalent flu antigens or trivalent flu antigens in combinations with the adjuvants: MF59 (1:1 in PBS), alum (200 µg/mouse), CpG (20 µg/mouse), R848 (25 µg/mouse) and Pam3CSK4 (10 µg/mouse). Mice were treated at time 0 (first immunization) and after 4 weeks (second immunization) and the sera were collected 2 weeks post-first or post-second immunization.

2.3.2 Immunization for microarray experiments

For *in vivo* microarray experiments 3 mice/group were treated for 6 h with the same compounds used for adjuvanticity experiments.

2.3.3 Immunization for flow cytometry experiments

For FACS analysis 3 mice/group were injected i.m. into both quadriceps again with the same compounds and draining lymph nodes were collected after 24 h to perform flow cytometric analysis of single cell suspensions.

2.3.4 Immunization for confocal microscopy experiments

For confocal microscopy analysis 3 mice/group were injected i.m. into both quadriceps with the same compounds used in the other experiments and muscles were collected at 6 h, 24 h and 72 h for cryosectioning.

2.4 Microarray Analysis

Microarray analysis was performed on whole muscle and LNs tissue collected 6 h after treatment.

2.4.1 Muscle RNA extraction and purification

At 6 h whole muscles were excised from mice and placed immediately on ice-cooled HBSS medium. Every muscle was then placed into 5 ml ice-cold TRIzol (Invitrogen). Muscles were homogenized with an Ultra-Turrax T25 for 30 s at maximum speed. Homogenized samples were incubated at room temperature for 10 min for complete dissociation of nucleoprotein complexes. Samples were transferred to 15 ml falcon tubes and 1 ml of ice-cold chloroform was added to each tube. The sample was vortexed for 15 s, incubated at room temperature for 2 min and then centrifuged for 15 min. The aqueous phase containing the RNA was immediately transferred to a new tube and 2.5 ml of ice-cold iso-propanol was added. Samples were incubated for 5 min at room temperature and then centrifuged for 10 min. The RNA precipitate formed a pellet, which was washed with 5 ml of 75% ethanol. Samples were centrifuged twice, for 5 min and 1 min respectively, to remove all the ethanol. All centrifugation steps were carried out at 9500 rpm at 4 °C. After drying the RNA pellets at room temperature for 10 min, the RNA was re-dissolved in 100 µl RNase-free water (Gibco, Cat. No. 10977-035), transferred in a 1.5 ml eppendorf tube. RNA concentration and integrity were assessed by the methods described below (see section 2.5).

At least 100 µg at 1 µg/µl of the RNA were purified using the RNeasy RNA purification columns (Qiagen). The RNA was mixed first with 350 µl of RLT buffer and then with 250 µl of 100% ethanol before loading onto the RNeasy mini column. After washing with 350 µl buffer RW1, 10 µl of DNase I (RNase-free DNase I set, Qiagen) diluted in 80 µl buffer RDD were added directly on the membrane for 15 min at room temperature for on-column DNase digestion. After washing with another 350 µl buffer RW1, 500 µl of RPE buffer were added and the columns were centrifuged at 10000 rpm for 2 min. Excess RPE buffer was removed by an additional centrifugation step for 1 min. The purified RNA was eluted with 30 µl of RNase-free water. After 1 min incubation at room temperature, the samples were centrifuged

for 1 min. To increase recovery efficiency and to increase the total concentration of RNA a second elution step with the same eluate was performed. All the centrifugation steps were all carried out at 10000 rpm for 30 s (unless stated). RNA concentration and integrity were assessed by the methods described below (see section 2.5).

2.4.2 Lymph nodes RNA extraction and purification

Inguinal draining lymph nodes of each mouse were collected in liquid nitrogen and immediately homogenized on ice in 600 µl RLT buffer, 1% β-mercaptoethanol using an Ultra Turrax T25 (IKA). The tissue lysates were transferred in a QIAshredder column (quiagen) and centrifuged. All centrifugation steps were carried out at 13000 rpm at 4 °C for 2 minutes. The flowthrough was mixed with 550 µl ethanol and the sample were transferred into the RNeasy RNA purification columns (Qiagen). The columns were washed with 700 µl RW1 buffer before on-column DNase digestion. For each column 10 µl of DNase I (Qiagen) was diluted with 70 µl of RDD buffer. The solution was loaded directly onto the membrane and incubated for 15 min at room temperature. After washing with 700 µl of RW1 buffer, columns were washed again with 500 ml of RPE buffer. The remaining RPE buffer was removed by an additional centrifugation step for 1 min. The purified RNA was eluted with 30 µl of RNase-free water. After 1 min incubation, the columns were centrifuged for 1 min. To increase the RNA yield and concentration, the elution step was repeated with the same eluate. The concentration and integrity of the RNA were measured with the methods described below (see section 2.5).

2.5 RNA quantification and quality assessment

2.5.1 Concentration measurement

RNA concentration was measured with the NanoDrop ND-1000 UV-Vis Spectrophotometer (Nanodrop Technologies). The “Nucleic Acid” application module was selected from the software menu. After blanking with MilliQ water, 2 μl of RNA sample was loaded directly onto the NanoDrop pedestal for concentration measurement. NanoDrop can measure RNA sample concentration up to 3700 $\mu\text{g}/\mu\text{l}$, without previous dilution.

2.5.2 Quality measurement

RNA quality was assessed using Bioanalyzer (Agilent)

When using the Bioanalyzer System (Bio-Rad), the samples were prepared by denaturing 3 μl of the RNA sample for 3 min at 70 °C followed by 5 min incubation on ice. The “gel” solution was prepared by centrifuging 600 μl RNA 6000 Nano Gel matrix gel at 1500 x g for 10 min, and was stored at 4°C until needed. The “gel-stain” solution was prepared by mixing 65 μl of filtered gel with 1 μl RNA 6000 Nano concentrate. The chip used was the RNA nano chips (Agilent). To prime the chip, 9 μl of gel-stain solution were added to the gel priming well and the chip was loaded on the priming station with pressure set to “B” and time to “1”. After priming, 9 μl gel-stain solution were loaded into the other well labelled GS, 9 μl filtered gel into the well labelled G, 5 μl RNA 6000 Nano marker (green cap) into each sample well (1–12) and into the well labelled L (ladder well), 1 μl denatured RNA ladder into the well labelled L and finally 1 μl denatured sample or 1 μl of DEPC-treated water into each of the 12 sample wells. The chip was vortexed for 1 min in the vortex station and then was placed in the electrophoresis station after priming following the Bio-Rad protocol. From the software, the Eukaryotic Total RNA assay was selected and the run was started.

2.5.3 RNA labelling and purification

Microarray samples were prepared using the quickamp labelling kit (Agilent), that results in Cyanine-3 (Cy3) RNA labelling allowing one-color microarray analysis. For each reaction, 400 ng of total RNA purified from a single muscle or lymph node pair were diluted in 6.3 μ l with RNase-free water, mixed to 1.2 μ l T-7 Promoter Primer (Agilent) and to 4 μ l of diluted Spike-Mix (Agilent RNA Spike-In Kit, One-Color) and incubated at 65 °C for 10 min to denature the primer and the template and immediately placed on ice for 5 min. The RNA was then retro-transcribed for 2 h at 40 °C in a circulating water bath with 8.5 μ l reaction mix/sample containing 4 μ l of 5X first strand buffer, 2 μ l of 0.1 M DTT, 1 μ l of 10 mM dNTP mix, 1 μ l of MMLV-RT and 0.5 μ l of RNaseOUT. The samples were then incubated for 15 min on ice. To generate the Cy3-labeled cRNA the sample was incubated again for 2 hrs with 57.6 μ l Transcription Master Mix containing 15.3 μ l nuclease-free water, 20 μ l 4X Transcription Buffer, 6 μ l 0.1M DTT, 8 μ l NTP mix, 6.4 μ l 50% PEG, 0.5 μ l RNaseOUT , 0.6 μ l Inorganic Phosphatase , 0.8 μ l T7 TNA Polymerase and with 2.4 μ l Cy3 that have to be lastly added to each sample.

The Cy3-labelled cRNAs were purified using the Qiagen's RNeasy mini spin columns. After addition of 20 μ l nuclease free-water, 350 μ l of RLT Buffer and 250 μ l ethanol 96% (mixing well by pipetting) the sample was loaded on a RNeasy mini spin column. The column was centrifuge for 30 sec at 4°C at 13000 rpm. The column was washed twice with 0.5 ml of Buffer RPE, followed by centrifugation for 30 sec at 4°C at 13000 rpm. The purified Cy3-labelled cRNA was eluted by adding 30 μ l RNase-free water followed by centrifugation for 30 sec at 4°C at 13000 rpm. 2 μ l of the eluate were loaded onto the NanoDrop instrument to assess the concentration of the cRNA and the efficiency of Cy3 dye incorporation. The samples were stored at -80 °C until needed.

2.5.4 Microarray Hybridization and Data Acquisition

Just before loading onto the microarray, Cy3-labeled cRNA samples were fragmented to shorten long RNA transcripts. The fragmentation samples were prepared by adding to 1.65 μ g of Cy3-labelled cRNA, 11 μ l of 10X blocking reagent (Agilent), nuclease-free water to bring

volume to 52.8 μl and, lastly, 2.2 μl 25X fragmentation Buffer (Agilent), vortexed and incubated at 60 °C for 30 min. The fragmentation reaction was stopped by adding 55 μl 2x GEx Hybridization Buffer HI-RPM (Agilent). After spinning for 1 min at 13000 rpm, 100 μl of the mix was loaded onto the array and hybridization was carried out for 17 h at 60 °C. The platform used was the 44k Agilent Whole Mouse Genome Microarray (Agilent). The Agilent whole mouse genome microarray includes more than 41,000 unique features, representing all known mouse genes and related transcripts. The microarray is generated using the ink-jet technology to build *in-situ* 60-mer oligonucleotide probes, which minimize cross-hybridization and allow high sensitivity.

After hybridization, the microarray sandwich was opened in wash buffer A, placed in a coplin jar and washed in 300 ml wash buffer A with stirring for 1 min at room temperature and then transferred and washed in 300 ml wash buffer B (pre-warmed at 37°C) for 1 min. Slides were then washed in Acetonitrile for 10 sec and finally in the Agilent Stabilization and Drying solution for 30 sec.

Images were acquired using the Agilent Scanner (Agilent) at a resolution of 5 μm in “tiff” format with extended dynamic range.

2.5.5 Microarray Data Analysis.

Raw images were initially analyzed using Agilent's Feature Extraction 10.7 Image Analysis Software in an automated, walkaway mode. The software automatically finds and places microarray grids, rejects outlier pixels, determines feature intensities and ratios, flags outlier pixels, and calculates statistical confidences. The files generated were then transferred to the BASE 1.2.17 database/analysis software. For each spot, local background was subtracted from the mean fluorescence intensity of Cy3 dye. Spot intensities were then normalized by the global median. Spots with a signal-to-noise (SNR) lower than 3 in the Cy3 channel or manually flagged for bad quality were filtered. The average intensity ratio of repeated spots from experimental repetitions was estimated by the LIMMA normalization and the accuracy and statistical significance of the observed ratios were determined using the Student's t test. Only genes having t-test p-values lower than 0.05 and average intensity ratios greater than 4 ($\log_2 \text{ratio} \geq |2|$) in one time point were selected.

The hierarchical clustering was performed with the TMEV 4.3.02 software on the log₂ transformed dataset applying the Euclidean distance matrix and the average linkage clustering method.

2.6 FACS Analysis of lymph nodes cell preparation

2.6.1 Lymph node cell preparation

Animals were sacrificed at 24 h after immunization and inguinal lymph nodes were extracted and kept in 1 ml physiological solution on ice. The organs were transferred into a Petri dish with 1 ml PBS, 5% FCS and cut with scalpel to little pieces. The solution containing the pieces was transferred into a 15 ml falcon tube, the Petri dish was additionally washed with 2-3 ml PBS, 5% FCS and the tube was centrifuged for 5 min at 3000 g at 4°C.

The supernatant was removed and the pellet was re-suspended in 0.5 ml RPMI medium (GIBCO) with 16 µl Collagenase D (ROCHE, stock 50 mg/ml) and 25 µl DNaseI (ROCHE, stock 10 mg/ml) for each lymph node. The samples were incubated for 15 min at 37°C under gentle agitation, transferred in the Gentlemax Dissociator (Miltenyi Biotech) for a rapid mechanical digestion and then again incubated for 15 min at 37°C under gentle agitation. After this second step of enzymatic digestion the samples were filtered through 70 µm cell strainer (BD Falcon) into 50 ml Falcon tube, transferred to 15 ml new falcon tube and then centrifuged for 5 min at 4°C at 3000 g. The supernatant was removed and the pellet was re-suspended in 250 µl PBS, 5% FCS. Cells were counted and transferred to 96 well round bottom plate for staining.

2.6.2 Lymph node cell staining

The aim of this staining was to investigate activation of different LNs cell population: cells were plated in duplicate and stained separately for T, B and NK cells and for Dendritic Cells.

1 x 10⁶ cells/well from LN single cell suspension were plated in duplicate in a round-bottom 96-well plate and after centrifugation at 300 g for 5 min at RT incubated for 20 min at room temperature in 20 µl/well of 20% rabbit serum. After washing, each LN suspension was stained with two antibody combinations. For T, B and NK cells staining we used anti-DX-5 biotin (BD Pharmingen), anti-TRAIL PE (eBioscience), anti-CD69 PerCP-Cy5.5 (eBioscience), anti-CD3 APC-eFluor780 (eBioscience), anti-CD19 A-700 (eBioscience) and Live/dead aqua (Invitrogen). For DCs, we used anti-CD11c PerCP-Cy5.5 and Live/dead aqua (Invitrogen). Anti-DX-5 biotin was detected with a second step incubation with Streptavidin PB (Invitrogen). All incubations were performed in 50 µl final volume for 20 min in the dark. Cells were re-suspended in 180 µl FACS buffer before acquisition on a FACS LSRII flow cytometer (BD Biosciences)

2.6.3 FACS analysis

At least 1 x 10⁶ events/LNs were acquired in the P1 gate (all events with FSC greater than 50). Data were analyzed using the FlowJo software.

Dead cells were excluded from the analysis with live/dead fixable staining kit (Invitrogen). After SSC vs. FSC gating on live cells to isolate lymphocytes (FSC^{low} SSC^{low}) and SSC vs. SSC-W gating to isolate single events, T cells were identified as CD3+ cells (B), B cells as CD19+ cells (C) and NK cells as DX5+ cells (D). CD69 or CD86 levels on these cell types were measured as mean fluorescence intensity of PerCP-Cy5.5 (CD69) and APC (CD86). SSC, side scatter; FSC forward scatter; SSC-W, side scatter width. Gating strategy can be seen in the Results section (figure 10 A-B-C-D)

2.7 Hemagglutination Inhibition test

All sera underwent a sample pre-treatment step. Sera were treated with DENKA receptor destroying enzyme (RDE, BIOGENETICS) in a 1:3 volume ratio for 18 h at 37°C. 6 volumes of PBS were added to get a final dilution of sample 1:10. Samples were inactivated at 56°C

for 30 min and stored at 4°C until use. Before use the virus antigen was titrated using a 50 µl serial tenfold dilutions of the stock vial. The virus working dilution (i.e. dilution factor to reach 4 Hemagglutinating Units (HAU) in a 25 µl volume) was calculated by dividing by 8 the previously determined stock titer, and was checked daily before the assay by the so-called “4 units test” Twofold serial dilutions of 25 µl pre-treated sera and positive control sera were treated with 25 µl of virus working dilution. After gentle shake, samples were incubated at room temperature for 60 min. 50 µl of turkey red blood cell (RBC) suspension were dispensed in each well and plates were again incubated at room temperature for 60 min. Results were recorded as soon as samples in the RBC control column started to form a “teardrop” of erythrocytes. For each sample the last well where inhibition of hemagglutination is observed was recorded and haemagglutinin titer calculated. The geometric mean of the duplicates is shown in the results.

2.8 ELISA test

Flu-specific, OVA-specific and TT-specific antibodies in the serum were measured by endpoint ELISA (204). MaxiSorp 96-well plates (Nunc, Cat. No. 439454) were coated for 2 h at 37°C with 2.5 µg/well of Flu antigen in 100 µl/well PBS (Sigma, Cat. No. G7641), 0.2 µg/well of TT antigen in 100 µl/well PBS and 2.5 µg/well of OVA antigen in 50 µl/well PBS followed by overnight incubation at 4°C. Wells were washed and blocked with 200 µl/well blocking buffer for 2 h at room temperature. After washing, 50 µl of samples or standard in 1:2 or 1:3 serial dilutions were incubated for 2 h at 37 °C. Standards were plated starting from a 1:200 dilution, serum samples were initially diluted 1:200. Plates were washed and incubated for 1 h at 37 °C with 100 µl/well of secondary antibody diluted 1:2000. The secondary antibodies used were: goat anti-mouse IgG (Southern Biotech, Cat. No. 1030-04), goat anti-mouse IgG1 (Southern Biotech, Cat. No. 1070-04) or goat anti-mouse IgG2a (Southern Biotech, Cat. No. 1080-04) all conjugated with alkaline phosphatase. After washing, 100 µl/well of *p*-nitrophenyl phosphate, disodium salt (pNPP) substrate (Sigma, Cat. No. A3469) were added to each well. The color developed during the enzymatic reaction of pNPP with alkaline phosphatase was detected after 35 min incubation in the dark at room

temperature by measurement of light absorbance at 405 nm using an ELISA microplate reader. ELISA titers were expressed as the reciprocal dilution that gave an OD higher than the average OD of the blanks plus 3 times the SD.

2.9 Confocal analysis

2.9.1 Muscles

Tissue sections of 5 μm thickness were thaw-mounted onto glass slides and air dried at room temperature.

Slides were fixed in a 4% formaldehyde solution at $-4\text{ }^{\circ}\text{C}$ for 10 minutes, following by an incubation with 3% BSA and 1% saponin in PBS for 20 minutes at room temperature. Slides were incubated with primary antibodies (utrophin and CD11b) for 1 h at RT. Then sections were washed with PBS 3% BSA and 1% saponin and incubated with secondary antibodies for Utrphin and CD11b and with ToPro3 to visualize nuclei for 2 h at RT, followed by two washing with PBS 3% BSA and 1% saponin and one wash with PBS.

Muscle fibers were detected with utrophin goat polyclonal IgG (Santa Cruz Biotechnology cat N. 7459) at a 1:50 dilution and chicken anti-goat AlexaFluor 488 (Molecular Probes, cat N. A21467) at 1:200 dilution. Cd11b was detected with rat anti-mouse Cd11b (AbD Serotec, cat N. MCA74GA) at 1:100 and goat anti-rat AlexaFluor 555 (Molecular probes, cat N. A21434) at 1:200 dilution. Nuclei were detected using ToPro3 (Molecular probes) at 1:1000 dilution. Slides were mounted with ProLong Gold antifade reagent (Invitrogen cat N. P36934), coverslipped and imaged on a LSM 710 microscope (Zeiss).

2.9.1 Lymph nodes

Tissue sections of 8 μm thickness were thaw-mounted onto glass slides and air dried at room temperature.

Slides were fixed in a 4% formaldehyde solution at -4 °C for 10 minutes, following by washing in PBS. Sections were then incubated with 3% BSA and 1% saponin in PBS for 20 minutes at room temperature, followed by an incubation with primary antibodies (GL7-biotin) for 1 h at RT. Following two washings with PBS 3% BSA and 1% saponin, slides were incubated with secondary reagents (a-rat AF555, IgG Dylight AF488, CD45R AF647) for approximately one hour at room temperature, followed by two washing with PBS 3% BSA and 1% saponin and one wash with PBS

GL7 was detected with Biotin anti-mouse/human CD45R (Biotin anti-mouse/human T and B cell activation antigen GL7; eBioscience, cat N. 13-5902-82) at a 1:400 dilution and goat anti rat-AlexaFluor 555 (Invitrogen, cat N. A21434) at 1:600 dilution. B220 was detected with Alexa-fluor 647 anti-mouse/human CD45R (eBioscience, cat N. 51-0452-82) at 1:800. IgG were detected using DyLight 488 AffiniPure F(ab')₂ Fragment Goat Anti-Mouse IgG (H+L) (Jackson ImmunoResearch) at 1:1200 dilution.

Slides were mounted with ProLong antifade reagent with DAPI (Invitrogen cat N. P36935), coverslipped and imaged on a LSM 710 microscope (Zeiss).

2.10 Mouse cytokine assay (MSD, Meso Scale Discovery)

MSD Cytokine Assays measure one to ten cytokines in a 96-well MULTI-ARRAY or MULTI-SPOT plate. The assays employ a sandwich immunoassay format where capture antibodies are coated in a single spot, or in a patterned array, on the bottom of the wells of a MULTI-ARRAY or MULTI-SPOT (Figure 1) plate.

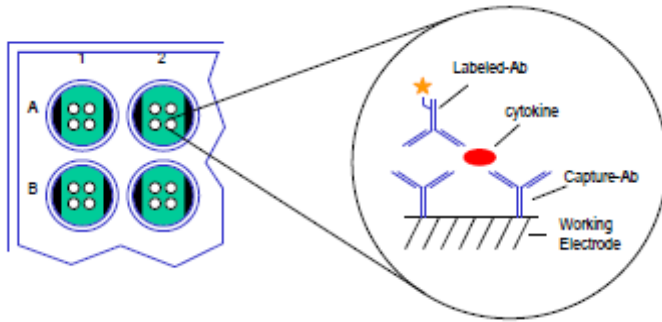


Figure 1: Cytokine capture antibody is pre-coated on specific spots of a 4-Spot MSD MULTI-SPOT plate. Calibrator solutions or samples are incubated in the MULTI-SPOT plate, and each cytokine binds to its corresponding capture antibody spot. Cytokine levels are quantitated using a cytokine-specific Detection Antibody labeled with MSD SULFO-TAGTM reagent.

A MULTI-SPOT plate will have an array of cytokine capture antibodies immobilized on the different spots. Any spot that is not coated with a specific capture antibody will be coated with BSA to reduce non-specific binding to that spot. For these experiments were used the 7-SPOT plates to identify the levels of cytokines IL-6, IL-10, KC, IL-1b, IFNg, TNFa and IL-12p70 in mouse sera.

All solid material was removed by centrifugation. Plasma prepared in heparin tubes commonly displays additional clotting following the thawing of the sample. It is important to remove any additional clotted material by centrifugation.

Calibrators were diluted in Diluent 4. The calibration curve was prepared as listed below to generate a standard curve from 10000 pg/mL to 2.4 pg/mL:

- 10000 pg/mL: add 10 μ L of the 1 μ g/mL stock solution to 990 μ L of Diluent 4. Use this high calibrator (10000 pg/mL) to prepare the standard curve following a 1:4 dilution series (as shown below).
- 2500 pg/mL: add 50 μ L of 10000 pg/mL combined high calibrator (10000 pg/mL) to 150 μ L of Diluent 4.
- 625 pg/mL: add 50 μ L of 2500 pg/mL calibrator to 150 μ L of Diluent 4.
- 156 pg/mL: add 50 μ L of 625 pg/mL calibrator to 150 μ L of Diluent 4.
- 39 pg/mL: add 50 μ L of 156 pg/mL calibrator to 150 μ L of Diluent 4.

- 9.8 pg/mL: add 50 μ L of 39 pg/mL calibrator to 150 μ L of Diluent 4.
- 2.4 pg/mL: add 50 μ L of 9.8 pg/mL calibrator to 150 μ L of Diluent 4.
- 0 pg/mL: 150 μ L of Diluent 4

Detection antibody solutions were kept in the dark as some antibodies may be light sensitive. The detection antibodies are provided premixed in solution at a 50X concentration (some vials may be labeled as 50 μ g/mL). The working detection antibody solution was prepared at 1X (or 1.0 μ g/mL). For each plate used, was diluted a 60 μ L aliquot of the stock Detection Antibody Mix into 2.94 mL of Diluent 5.

The Read Buffer was diluted 1:2 in deionized water to make a final concentration of 2X Read Buffer T. 10 mL of stock Read Buffer T (4X) was added to 10 mL of deionized water for each plate.

As first step 25 μ L of Diluent 4 were dispensed into each well to the bottom of the plate. A slight tap may be necessary to allow the fluid to settle to the bottom. The plate was sealed with an adhesive plate and incubated for 30 minutes with vigorous shaking (300-1000 rpm) at room temperature. 10 μ L of each Calibrator or Sample Solution were dispensed into a separate well of the MSD plate. The plate was sealed with an adhesive plate and incubated for 2 hours with vigorous shaking (300-1000 rpm) at room temperature. Then the plate was washed with PBS + 0.05% Tween-20 and 25 μ L of the 1X Detection Antibody Solution were dispensed into each well of the MSD plate. The plate was sealed again and incubated for 2 hours with vigorous shaking (300-1000 rpm) at room temperature.

The plate was washed with PBS + 0.05% Tween-20 and 150 μ L of 2X Read Buffer T were added to each well of the MSD plate. The plate was analyzed on the SECTOR Imager. Plates may be read immediately after addition of Read Buffer.

3. Results

3.1 The activity of different vaccine adjuvants depends on the antigen.

To test the adjuvant activity of different compounds, the TLR-independent adjuvants MF59 and alum, the TLR9 agonist CpG, the TLR7/8 agonist R848 and the TLR2 agonist Pam3CSK4, BALB/c mice were immunized i.m. with tetanus toxoid antigens, with OVA antigen or with seasonal flu antigens, either alone or in combination with all the adjuvants listed.

8 mice/group were injected with 50 µl/quadriceps in both quadriceps and sera were collected 2 weeks post first and 2 weeks post second immunization and used to measure antibody titers and HI titers to flu. PBS-injected mice were used as control group for MF59, alum and CpG, while 1% DMSO-treated mice were the control group for R848 and Pam3CSK4.

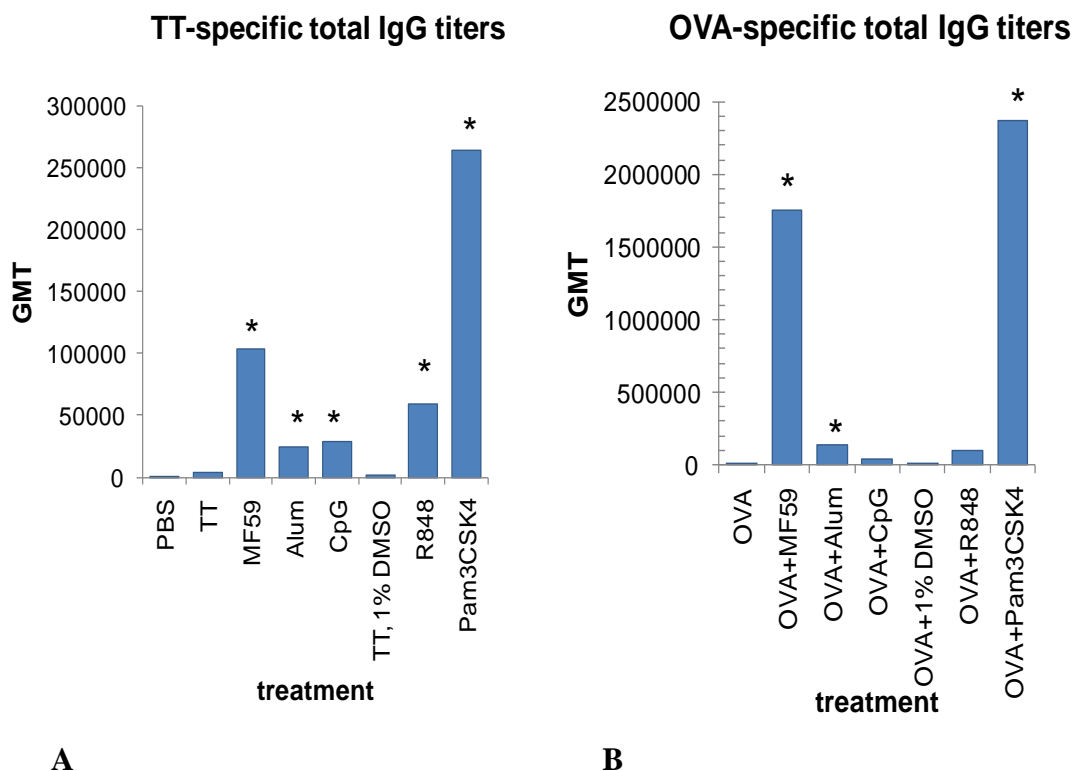


Figure 1: (A) total IgG titers after immunization with tetanus toxoid antigens either alone or in combination with MF59, alum, CpG (all in PBS), Pam3CSK4 or R848 (in PBS, 1% DMSO). **(B)** total IgG titers after immunization with OVA antigen either alone or in combination with MF59, alum, CpG (all in PBS), Pam3CSK4 or R848 (in PBS, 1% DMSO). The values are shown as geometric mean titer (GMT) over 8 mice. Significance was calculated by student's t-test, *p-value \leq 0.05. The data is representative of 2 different experiments.

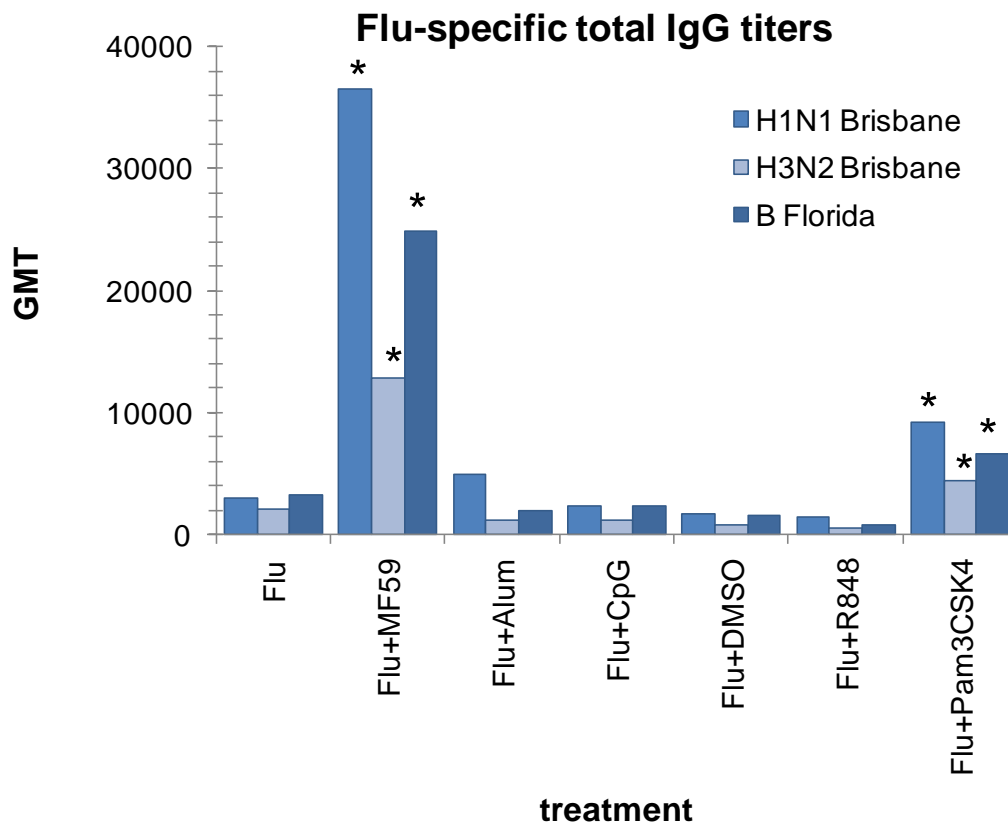


Figure 2: total IgG titers after immunization with seasonal trivalent flu either alone or in combination with MF59, alum, CpG (all in PBS), Pam3CSK4 or R848 (in PBS, 1% DMSO).

The values are shown as geometric mean titer (GMT) over 8 mice. Significance was calculated by student's t-test, *p-value \leq 0.05. The data is representative of 2 different experiments.

Analysis of total IgG titers (fig.1 and fig.2) showed that, compared to their controls, all adjuvants, induced significant total IgG titers to TT antigens (fig.1A) and that MF59, alum and Pam3CSK4 induced significant total IgG titers to OVA (fig.1B). On the other hand, only MF59 and, to a lesser extent, Pam3CSK4 induced significant total IgG titers to flu antigens (fig.2). HI titer data reflected what was seen for total IgG titers (fig. 3): MF59 and Pam3CSK4 were the only adjuvants that induce significant HI titers to flu antigens.

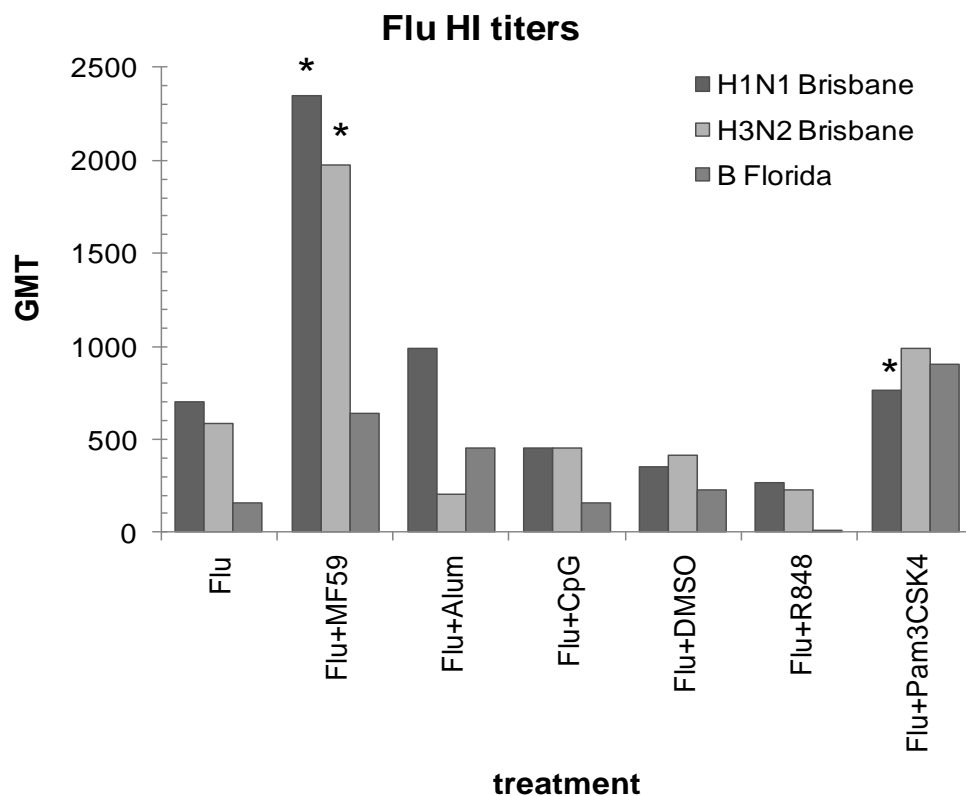
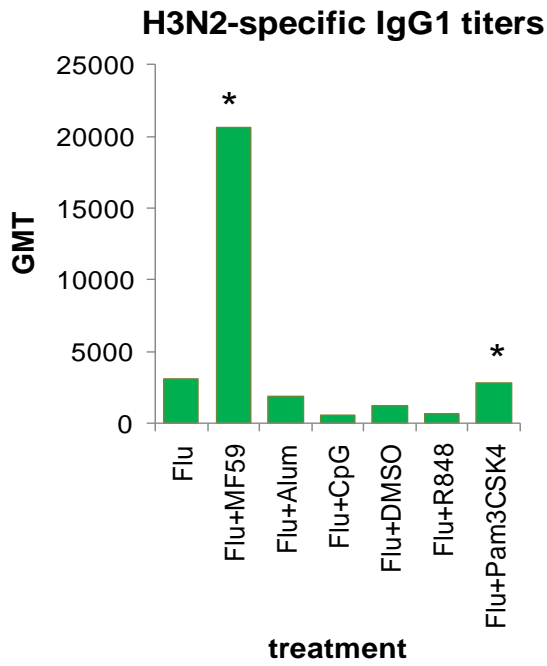
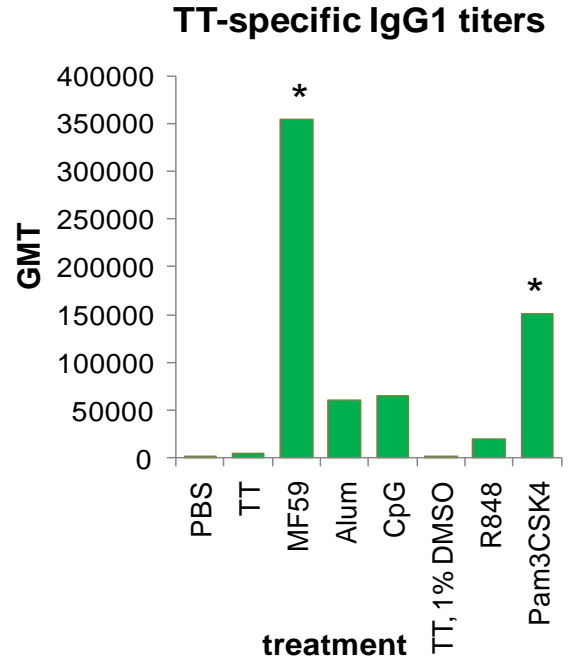


Figure 3: HI titers after immunization seasonal trivalent flu either alone or in combination with MF59, alum, CpG (all in PBS), Pam3CSK4 or R848 (in PBS, 1% DMSO).

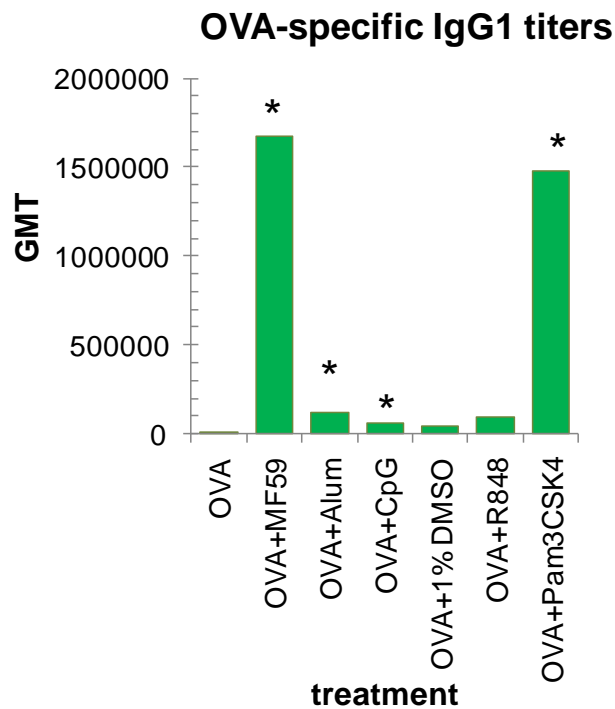
The values are shown as geometric mean titer (GMT) over 8 mice. For H1N1 and H3N2 significance was calculated by student's t-test, *p-value ≤ 0.05 . The data is representative of two different experiments. HI titers to B were measured over 2 pools of 4 mice/pool, therefore significance was not assessed.



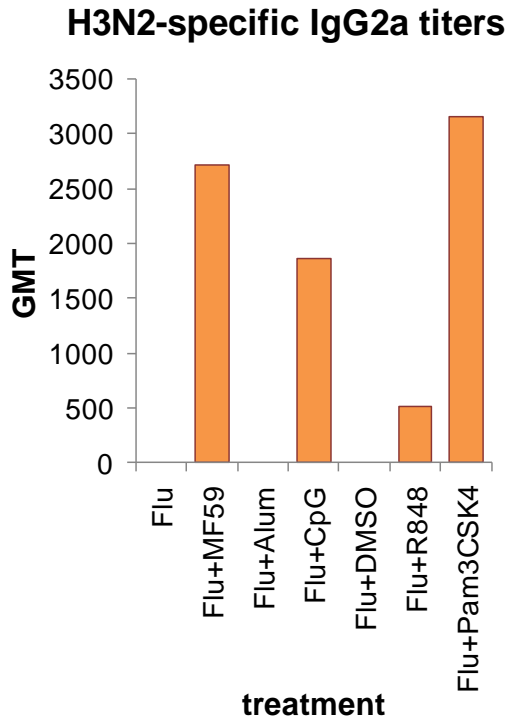
A



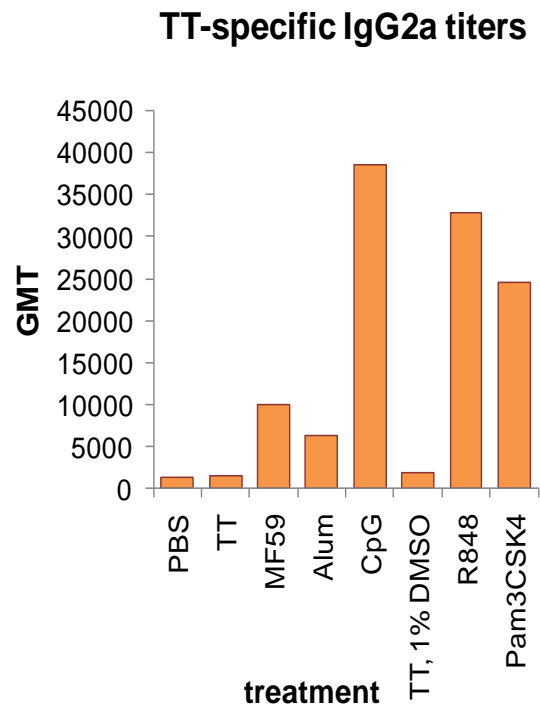
B



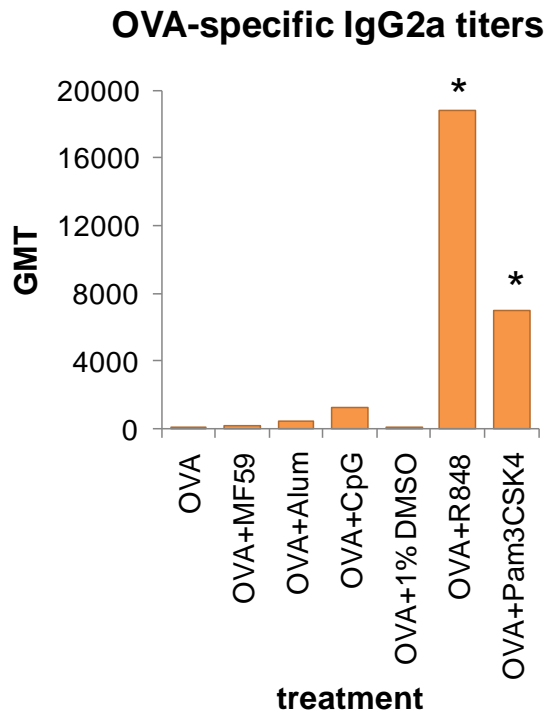
C



D



E



F

Figure 4: IgG1 (A-B-C) and IgG2a (D-E-F) titers after immunization with H3N2 flu antigen (A-D), with tetanus toxoid antigens (B-E), or with OVA antigen (C-F) either alone or in combination with MF59, alum, CpG (all in PBS), Pam3CSK4 or R848 (in PBS, 1% DMSO). The values are shown as geometric mean titer (GMT) over 8 mice. Significance was calculated by student's t-test, *p-value \leq 0.05.

Analysis of antibody isotypes showed that MF59 induced significant IgG1 titers to all antigens (fig 4A-C). This is not surprising as MF59 is known to induce a Th2-biased response in BALB/c mice [46-47]. Moreover MF59 also induced significant IgG2a to H3N2 (fig. 4D). Pam3CSK4 induced both IgG1 and IgG2a to all antigens, not statistically significant only in the case of IgG2a to TT (fig. 4E). R848 was not able to induce IgG1 (fig. 4A-C), but induced high level of IgG2a to TT and OVA (fig. 4E, 4F). CpG induced low levels of IgG1 to TT (fig. 4B) and OVA (fig. 4C), while it strongly enhanced IgG2a to H3N2 and TT (4D-E). Alum only induced low but significant IgG1 titers to OVA (fig. 4C), but was not able to induce IgG2a in combination with any of the antigens (fig. 4D-F)

3.2 MF59 is the strongest activator of gene transcription in the mouse muscle, while R848 activate gene expression in the LNs.

We performed microarray analysis in order to identify gene-signatures that might correlate with flu adjuvanticity. We analyzed, through microarray, the transcriptional profiles of splenocytes (*in vitro*), mouse muscles and draining lymph nodes (*in vivo*), after treatment with the same adjuvants tested in the adjuvanticity experiments (see fig. 1-4).

To dissect innate immune gene signatures induced by i.m. injection of adjuvants, we decided to test the transcription profiles induced by each adjuvant at an early time point: 6 h. In order to evaluate a possible effect of the antigen in combination with the adjuvant on the transcriptional profile of the adjuvant done, we tested the expression profile of trivalent flu,

trivalent flu plus MF59 or MF59 alone. Data showed that flu antigens alone do not induce transcriptional event *in vitro/vivo* and that the addition of the antigen to the adjuvant doesn't alter the expression profile of MF59 alone.

In the following table (table 1) we can observe the genes significantly regulated in the various tissues 6 h after treatment with the different adjuvants. *In vitro*, in mouse splenocytes, the TLR agonists, CpG, R848 and Pam3CSK4, strongly activated gene expression. Indeed splenocytes express toll-like receptors on their surface suggesting a direct activation of these cells after treatment with TLR agonists. On the contrary, as expected, the TLR-independent adjuvants did not have almost any transcriptional activity *in vitro*. *In vivo*, MF59 was the strongest modulator of transcriptional events at the injection site (970 regulated genes in contrast to only 2 genes modulated in the draining LNs). The TLR7/8 agonist R848 strongly regulated gene expression in the draining lymph nodes (1177 regulated genes *vs* 376 genes in the muscle).

Genes selected having fold change $\geq 4 $ and pval ≤ 0.05 in at least one condition				
Treatment (6 h)	immunization	Mouse splenocytes	Muscle	Draining LNs
MF59	(1:1 <i>in vivo</i> , 1:300 <i>ex vivo</i>)	13	970	2
Alum	(200 μg <i>in vivo</i>)	53	551	25
CpG	(20 μg <i>in vivo</i>)	1315	167	1
R848	(10 μg <i>in vivo</i> , 1 mM <i>ex vivo</i>)	949	376	1177
Pam3CSK4	(25 μg <i>in vivo</i> , 5 mM <i>ex vivo</i>)	510	99	75

Table 1: Table of number of genes selected (in the three different tissues and after injection the various adjuvants) having fold change $\geq |4|$ and $pval \leq 0.05$ in at least one condition.

From the significantly regulated genes we selected interesting gene clusters: the cytokine and chemokine genes and the IFN-related genes.

In vitro, in mouse splenocytes, (fig. 5A, 5B) as expected, the TLR agonists, CpG, R848 and Pam3CSK4, strongly activated cytokine and chemokine genes. On the other hand, the TLR-independent adjuvants did not regulate these genes, suggesting that they are not directly activating immune cells *in vitro*. *In vivo* their strong adjuvanticity might result from indirect activation of DCs through different mechanisms including activation of other cell types such as stromal cells. The same can be observed for IFN-related genes. As expected CpG and R848 were stronger inducers of IFN genes compared to MF59, alum and TLR2 agonist Pam3CSK4.

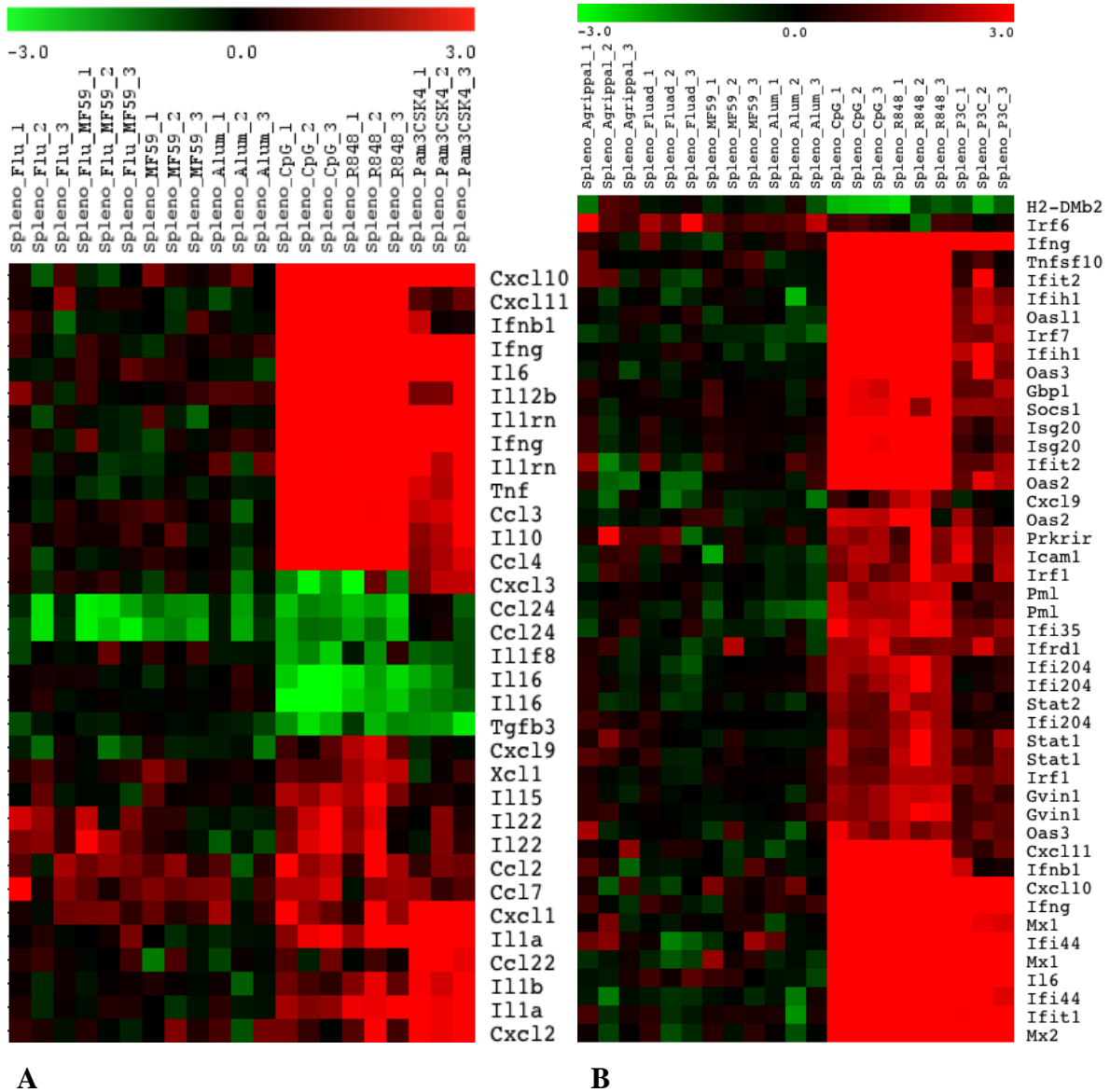
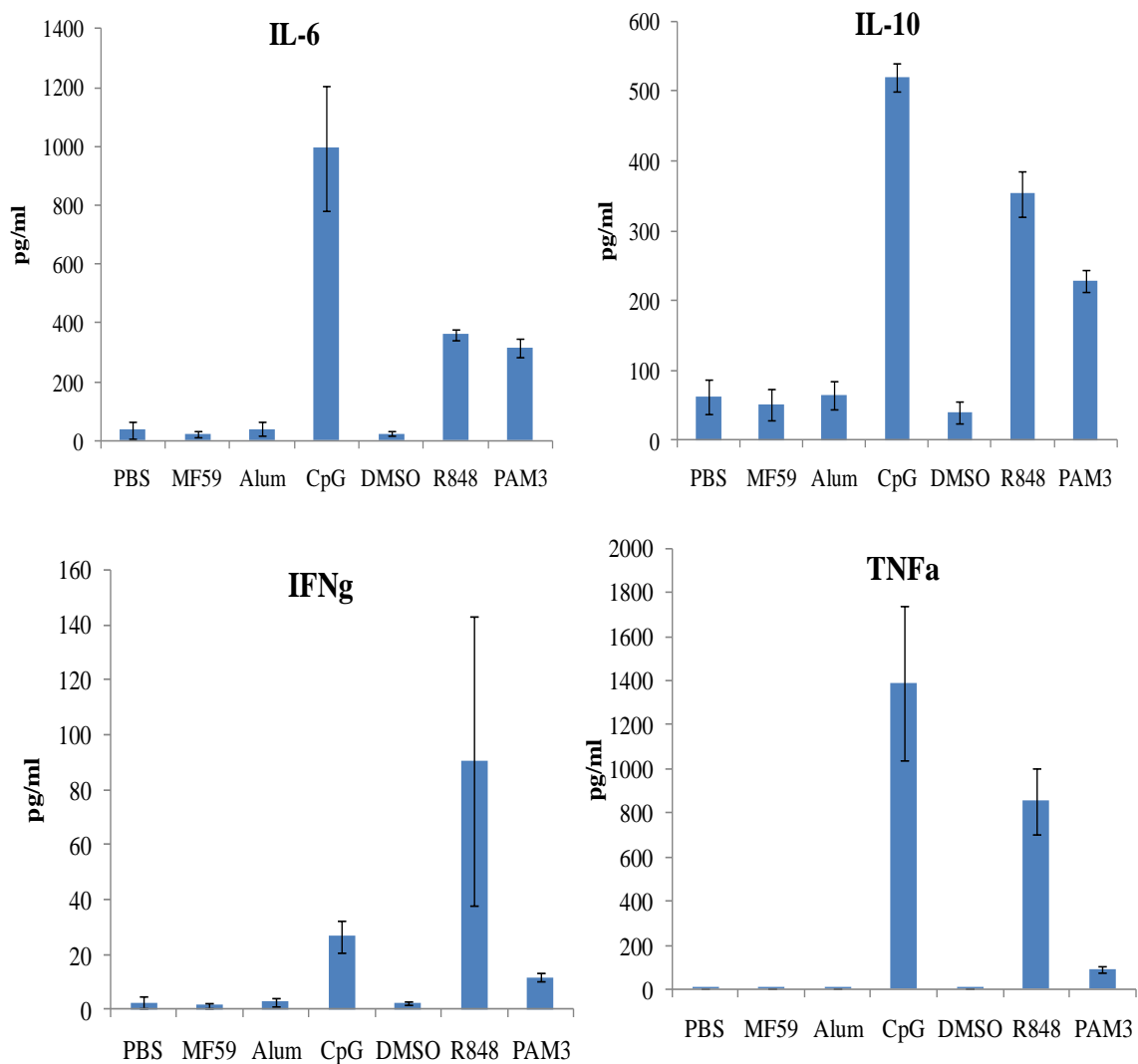


Figure 5: Expression profile 6 h after stimulation of mouse splenocytes with flu antigens, flu antigens plus MF59, MF59, alum CpG, R848 or Pam3CSK4. Each row represents a single gene, each column represents a single mouse. Each treatment is shown in triplicate. A subset of genes encoding for cytokine and chemokine (**A**) or interferon and interferon regulated genes (**B**) have been hierarchically clustered using the Euclidean algorithm. Genes significantly regulated have fold change ≥ 4 and $pval \leq 0.05$ in at least one condition. The log₂ scale ranges from -3, green, down-regulated genes to +3, red, up-regulated genes.

Analysis of cytokines protein levels in the serum at 6 h by a multianalyte cytokines detection system (Mesoscale Discovery) showed that MF59 and alum did not induce secretion of any of the cytokines tested. While CpG was a strong inducer of TNF α , IL-6, IL-12 and IL-10, Pam3CSK4 induced lower levels of the some cytokines, with the exception of TNF α (not produced) and KC (strongly regulated). R848 strongly induced IFN γ , IL-12, IL-10, TNF α and, to a lesser extent, IL-6 and KC (fig.6). These data confirmed microarray analysis *in vitro* (fig.5A-B), showing that only the TLR-dependent adjuvants were able to induce systemic cytokines production.



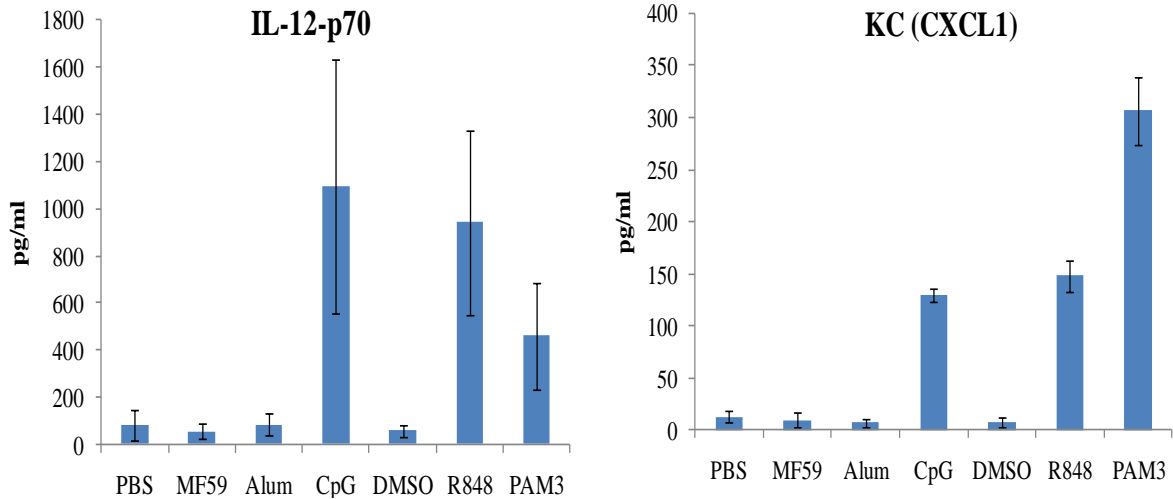


Figure 6: Concentration (pg/ml) of indicated cytokines secreted by mouse splenocytes 6 h after stimulation with PBS, MF59, alum, CpG, 1% DMSO, R848 or Pam3CSK4. SD were calculated based on at least three independent experiments.

In vivo, in the mouse muscle (fig. 7A, 6B), we observed that MF59 was the strongest modulator of cytokine and chemokine genes such as Il5, Il4, Ifng, Tnfa. Moreover, we observed that all adjuvants, with exception of R848, activated a core sets of important genes including Il6, Il1b, Ccl2 and Cxcl2. Interestingly, R848 activated only Cxcl13 and the Ifn-responsive chemokines Cxcl9, Cxcl10 and Cxcl11.

Analysis of the interferon response showed that CpG, as expected, strongly induced IFN signalling and IFN responsive genes. In contrast to the other adjuvants, R848 was also a strong inducer of these genes. Indeed stimulation of TLR7 and TLR9 is known to induce type I IFN response [48-49].

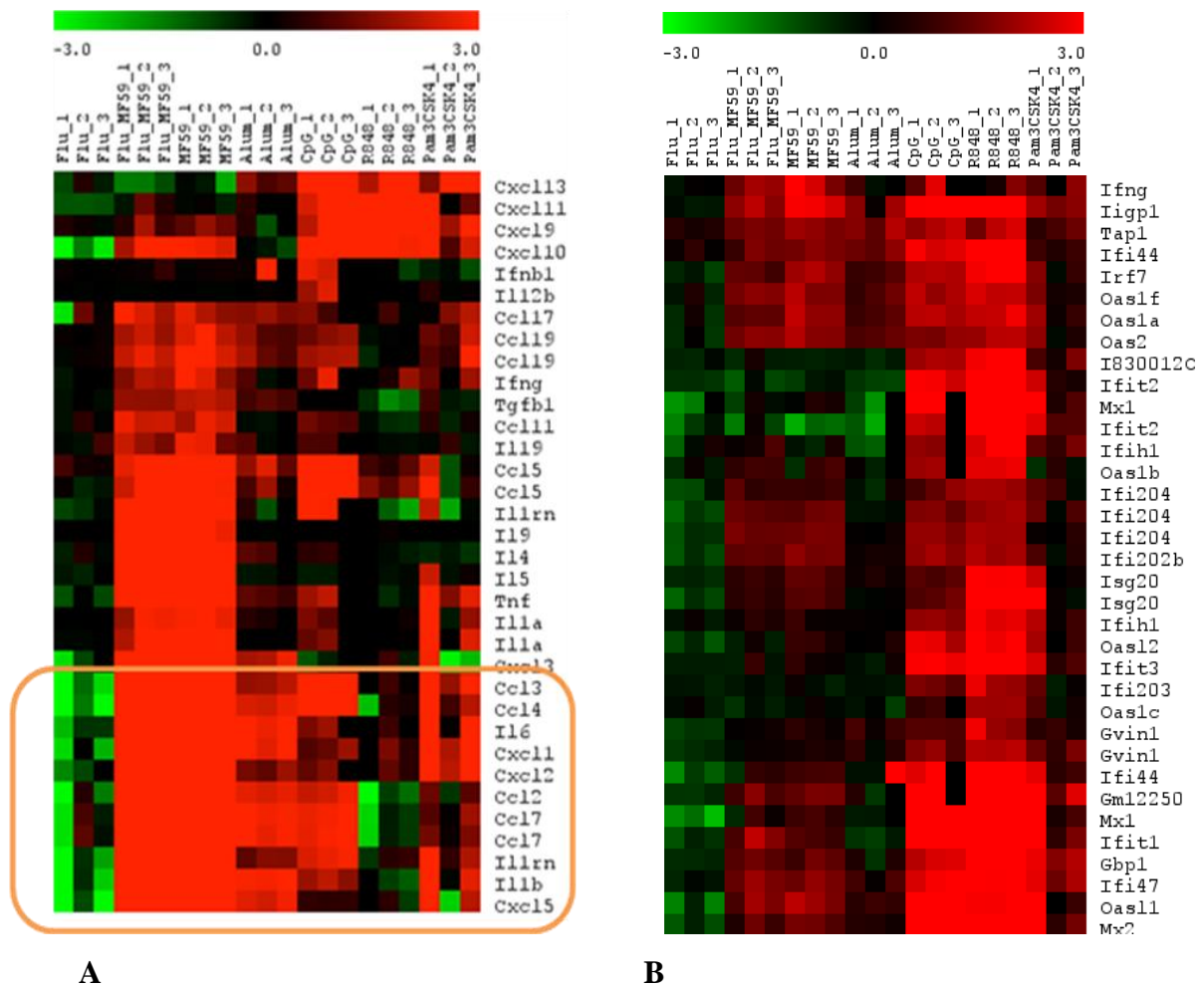


Figure 7: Expression profile 6 h after injection in mouse muscle. Genes encoding for cytokines and chemokines (A) or interferon and interferon regulated genes (B) have been hierarchically clustered using the Euclidean algorithm.

Analysis of gene expression patterns in the draining lymph nodes showed very different results compared to the muscle (fig. 8A, 8B). Interestingly R848 was the strongest activator of cytokine and chemokine genes in the LNs, with some effect also given by Pam3CSK4. Moreover R848 was the only activator of IFN-related genes. MF59, alum and CpG did not activate either of these gene classes. At least not over the threshold level we used to select significantly regulated genes.

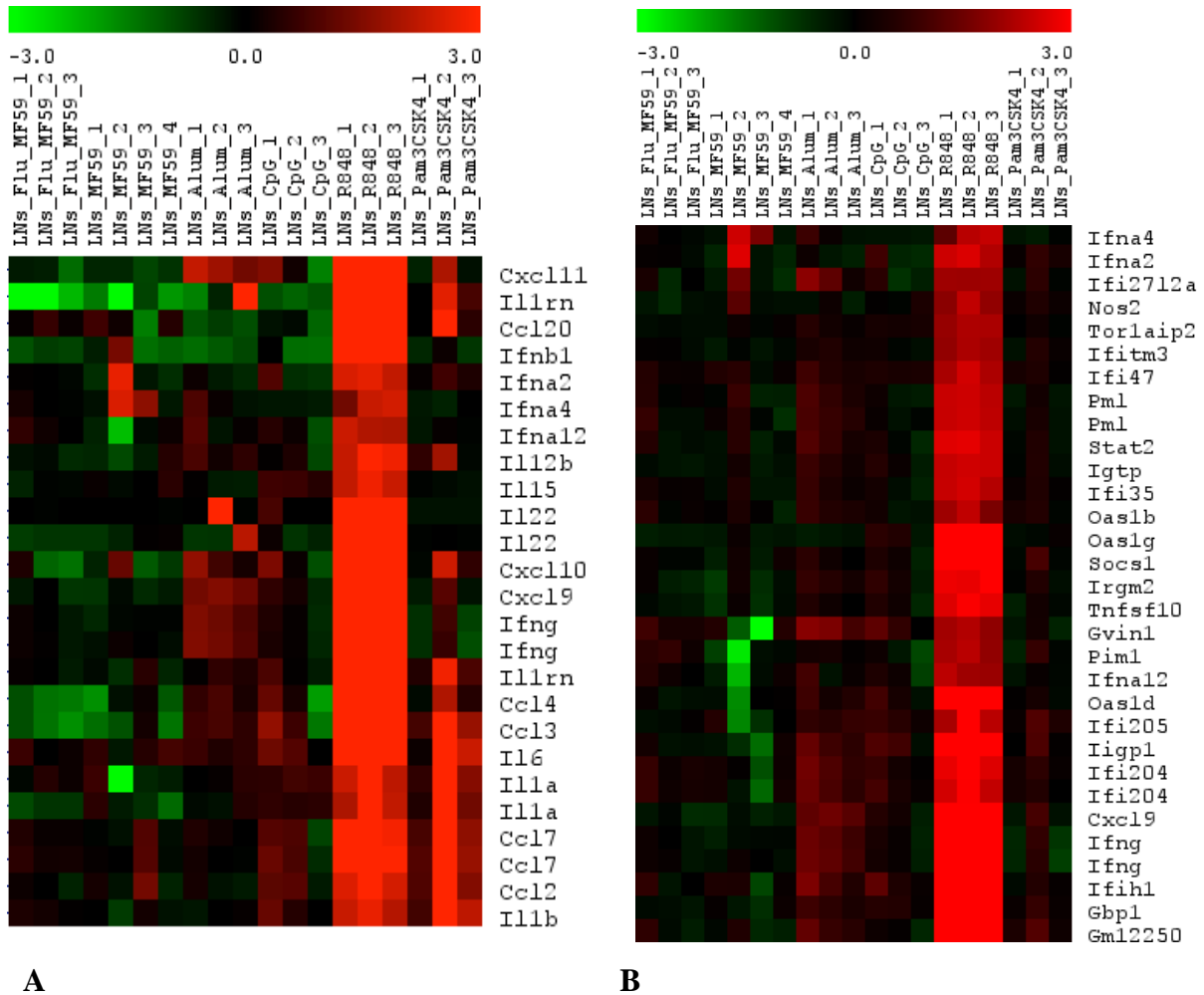


Figure 8: Expression profile 6 h after injection in mouse draining lymph nodes. Genes encoding for cytokines and chemokines (**A**) or interferon and interferon regulated genes (**B**) have been hierarchically clustered using the Euclidean algorithm.

3.3 R848 induces CD69 and CD86 expression in the LNs on T/NK and B cells respectively.

To confirm some data obtained by previous experiments, the four biomarkers CD69, CD86, Granzyme B and Tnsf10/TRAIL, shown to be upregulated in the lymph nodes by microarray analysis after R848 treatment, were selected in order to investigate the activation status of different lymph node cell populations (fig. 9).

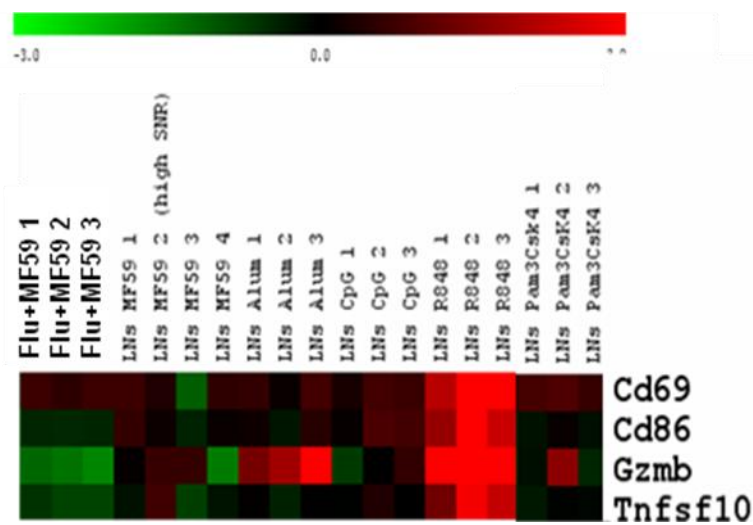
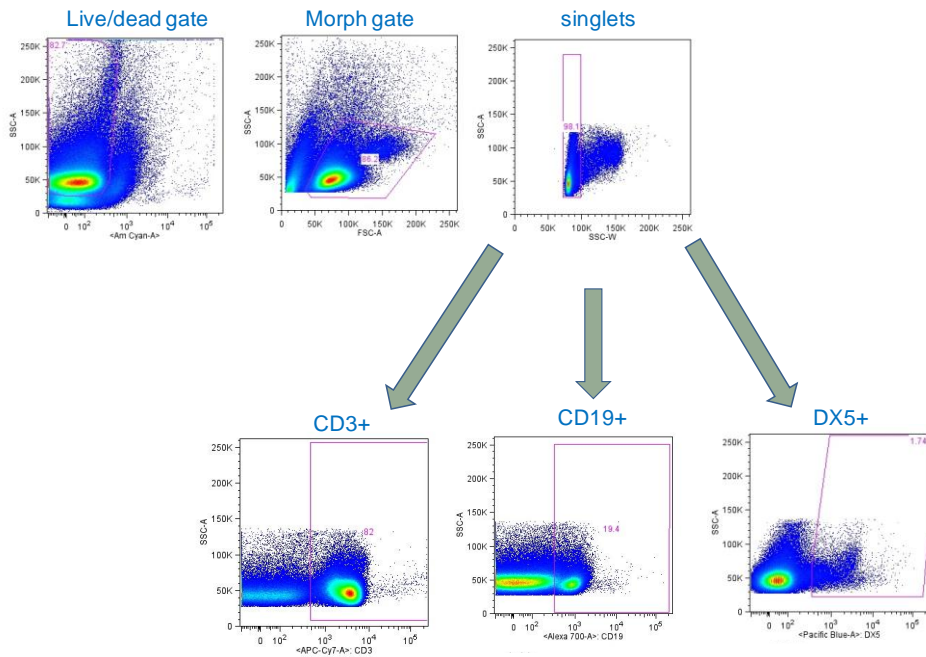
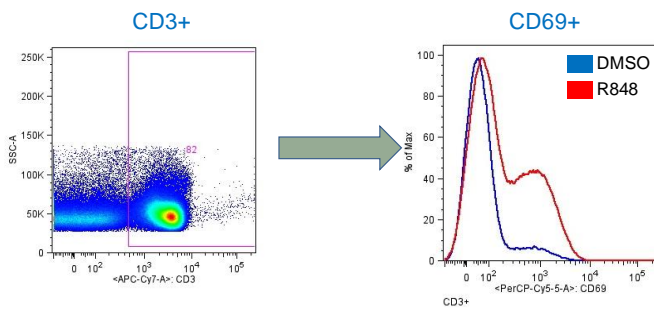
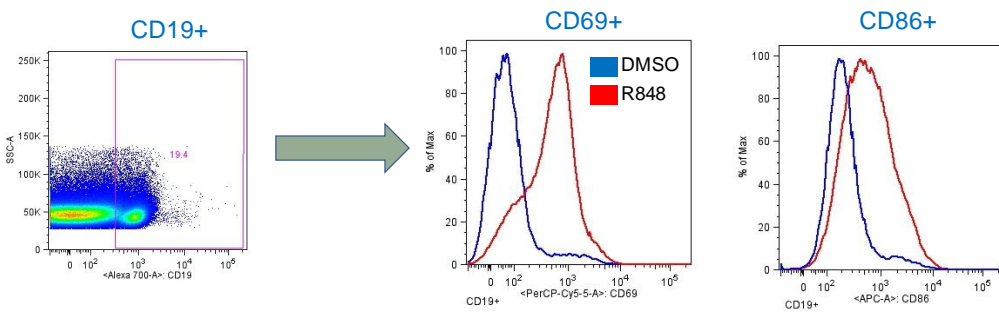


Figure 9: microarray expression of the four biomarkers CD69, CD86, Granzyme B and Tnfsf10/Trail in the draining lymph nodes 6 h after treatment with the various adjuvants.

We performed a multicolor FACS staining to identify the biomarker protein expression in the different cell types isolated from draining lymph nodes 24 h after i.m. injection with the different adjuvants (fig. 10).

A**B****C**

D

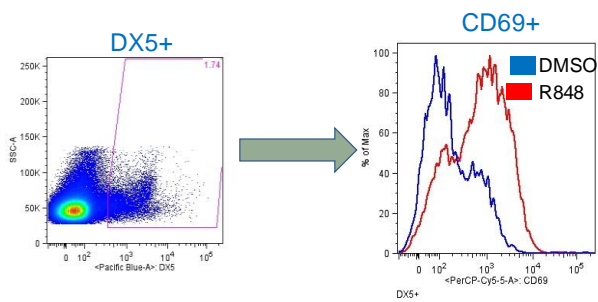


Figure 10: Gating strategy used for multicolor-flow cytometric analysis of LN cells. (A) Dead cells were excluded from the analysis with live/dead fixable staining kit (Invitrogen). After SSC vs. FSC gating on live cells to isolate lymphocytes ($FSC^{low} SSC^{low}$) and SSC vs. SSC-W gating to isolate single events, T cells were identified as CD3+ cells (B), B cells as CD19+ cells (C) and NK cells as DX5+ cells (D). CD69 or CD86 levels on these cell types were measured as mean fluorescence intensity of PerCP-Cy5.5 (CD69) and APC (CD86). SSC, side scatter; FSC forward scatter; SSC-W, side scatter width.

Flow cytometric analysis of LN single cell suspensions showed, in agreement with microarray data, that R848 was the only compound inducing up-regulation of CD69 on T cells (fig. 11A), B cells (fig. 11B) and natural killer (NK) cells (fig. 11C).

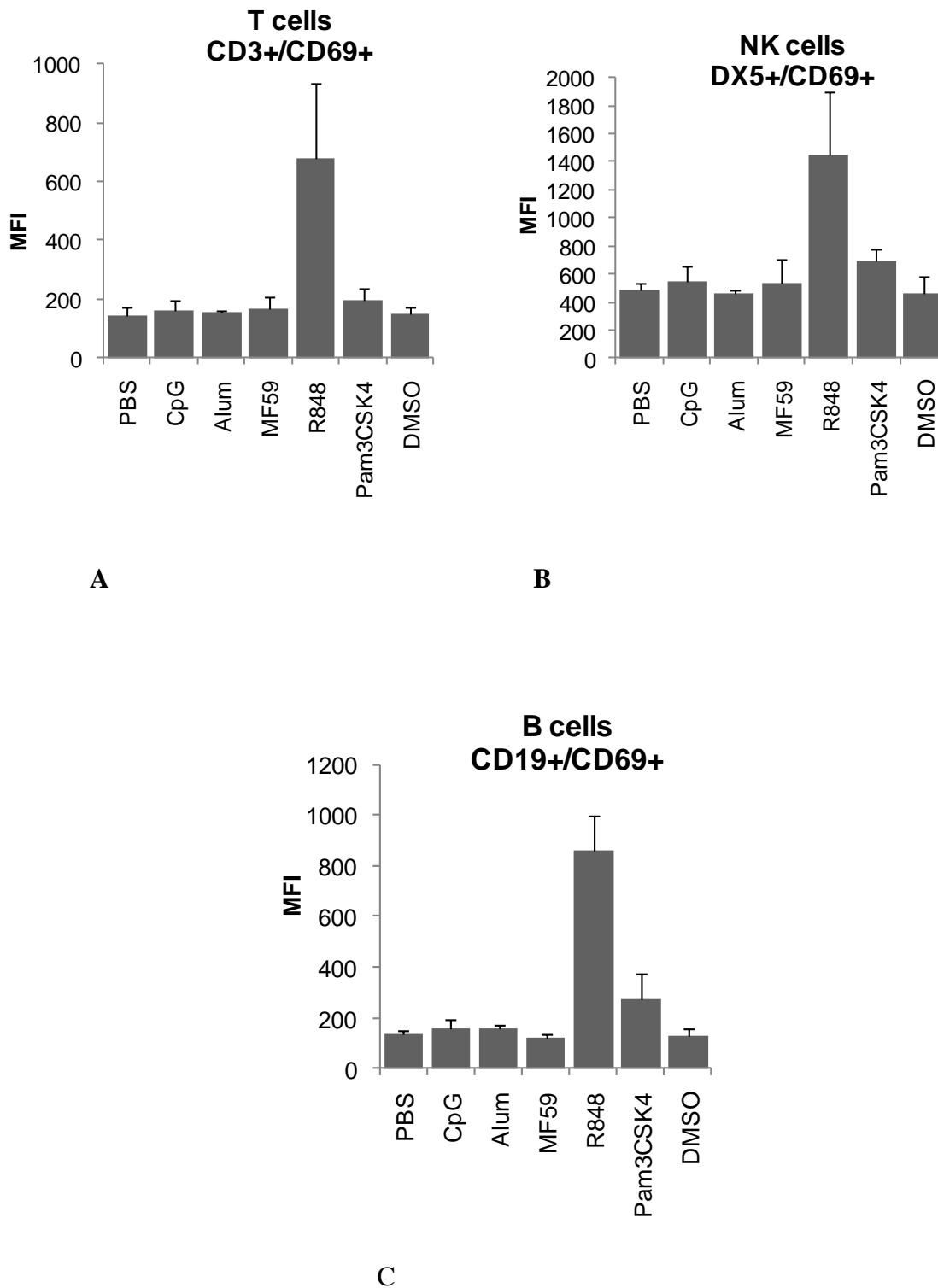


Figure 11: Multi-color flow cytometric analysis of CD69 on T (A), B (B) and NK cells (C) isolated from the draining LNs 1 day after i.m. injection with the different adjuvants. In the graph the mean fluorescence intensity of CD69 on the relative subsets is shown. SD were calculated based on at least three independent experiments.

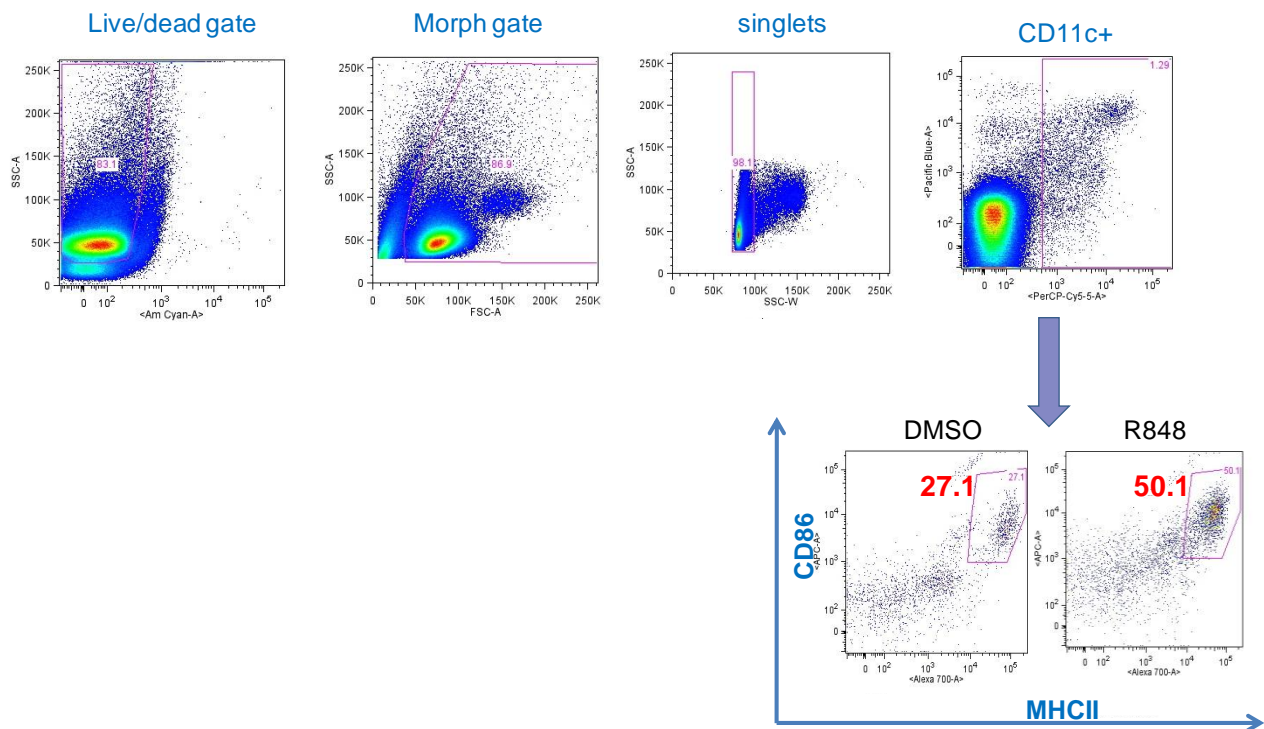


Figure 12: Gating strategy applied to multicolor-flow cytometric analysis of LN cells. Dead cells were excluded from analysis with live/dead fixable staining kit (Invitrogen). After SSC vs. FSC gating on live cells to isolate lymphocytes (FSC^{low} SSC^{low}) and SSC vs. SSC-W gating to isolate single events, DCs cells were identified as CD11c+ cells having high FSC and low/intermediate SSC. Within this population we compared the number of cells expressing CD86 and high level of MHC class II molecules after treatment with the various adjuvants. SSC, side scatter; FSC forward scatter; SSC-W, side scatter width.

In addition R848 induced the expression of CD86 in B cells (fig 13) and increased the number of DCs (CD11c+/CD11b+) expressing CD86 and high level of MHC class II molecule (fig. 14).

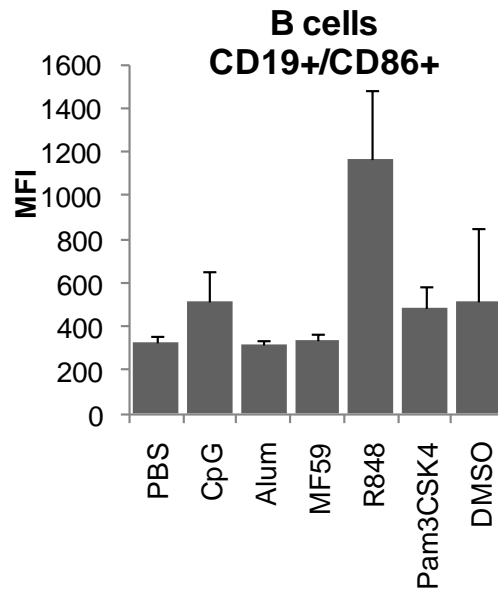


Figure 13: Multi-color flow cytometric analysis of CD86 on B cells isolated from the draining LNs 1 day after i.m. injection with the different adjuvants. In the graph the mean fluorescence intensity of CD86 on the relative subsets is shown. SD were calculated based on at least three independent experiments. SSC, side scatter; FSC forward scatter; SSC-W, side scatter width.

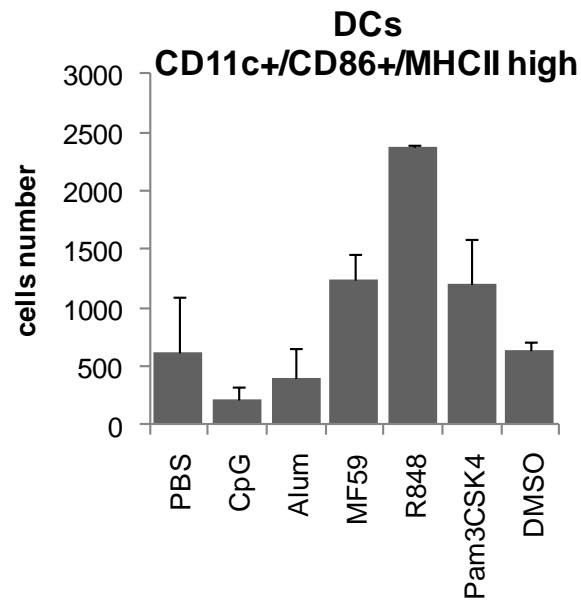


Figure 14: Multi-color flow cytometric analysis of MHC class II expression on DCs isolated from the draining LNs 1 day after i.m. injection with the different adjuvants. The bars represent the number of DCs expressing CD86 and high level of MHCII molecules for each treatment. SD were calculated based on at least three independent experiments. SSC, side scatter; FSC forward scatter; SSC-W, side scatter width.

These results confirmed data obtained by microarray analysis of LNs at 6 h: there was a correlation between mRNA expression and protein production for these activation markers, suggesting an activation of the lymph node after treatment with R848, not observed with other adjuvants.

3.4 MF59 activates transendothelial migration genes at the injection site.

An unbiased analysis of our gene data set highlighted, another interesting cluster of genes: belonging to the transendothelial migration pathway these genes appeared significantly expressed at 6 h in the muscle after treatment with MF59 (fig. 15). Some genes including Itgam, Icam-1, Vcam-1 were also regulated by CpG and Pam3CSK4.

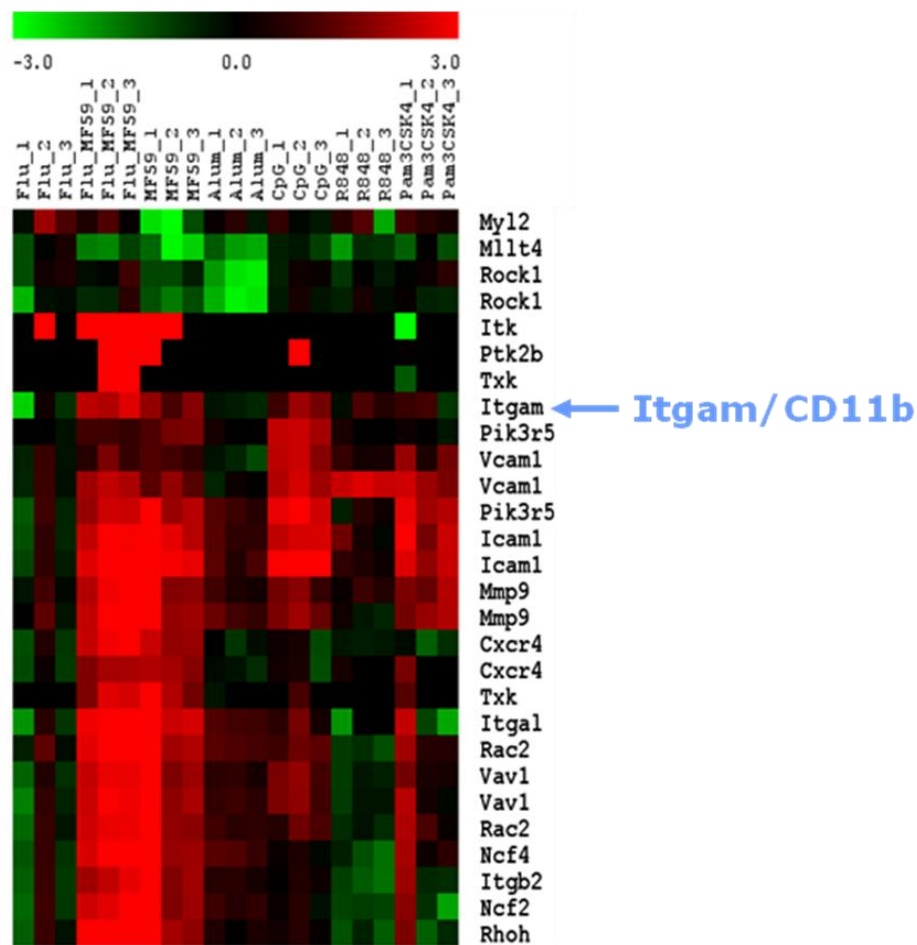


Figure 15: Expression profile of significantly expressed genes belonging to transendothelial migration pathway (KEGG HSA04670) in the muscle 6 h after treatment with the various adjuvants.

These results suggested that MF59, in contrast to the other adjuvants tested in these experiments, could lead to a strong and early cell recruitment from the bloodstream to the muscle, that happens very early. Moreover MF59 strongly activated chemokine and cytokine receptor genes, as shown in the figure 16.

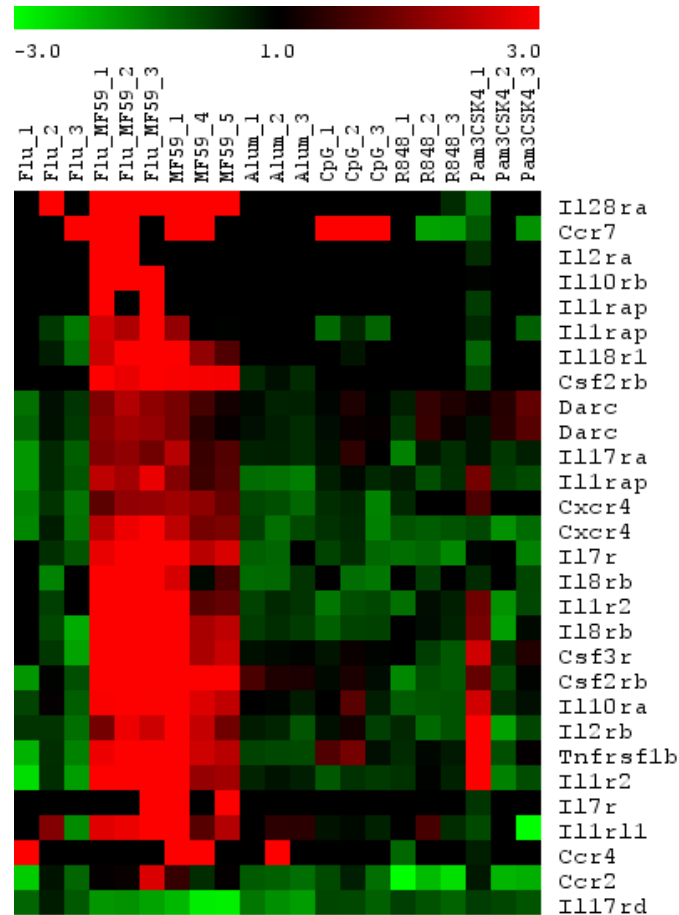


Figure 16: Expression profile 6 h after injection in mouse muscle. Genes encoding for cytokines and chemokines receptors have been hierarchically clustered using the Euclidean algorithm.

We selected CD11b/Itgam, among the genes encoding chemoattractants or adhesion molecules, as a marker to investigate local cell recruitment events after i.m. adjuvant injection at 6 h, 24 h and 4 days. We performed confocal immunofluorescence analysis of muscle cryosections. The structure of the muscle was visualized by using an antibody specific for utrophin, a cytoskeleton protein playing a role in activating the cytoskeleton to the plasma membrane and located in the sarcolemma of the muscle cells. Nuclei were visualized by ToPro 3 a cyanine nucleic acid stain allowing DNA detection.

At the early time point (6 h) we observed (fig. 17) that MF59 and slightly Pam3CSK4, can draw influx of CD11b+ cells at the injection site.

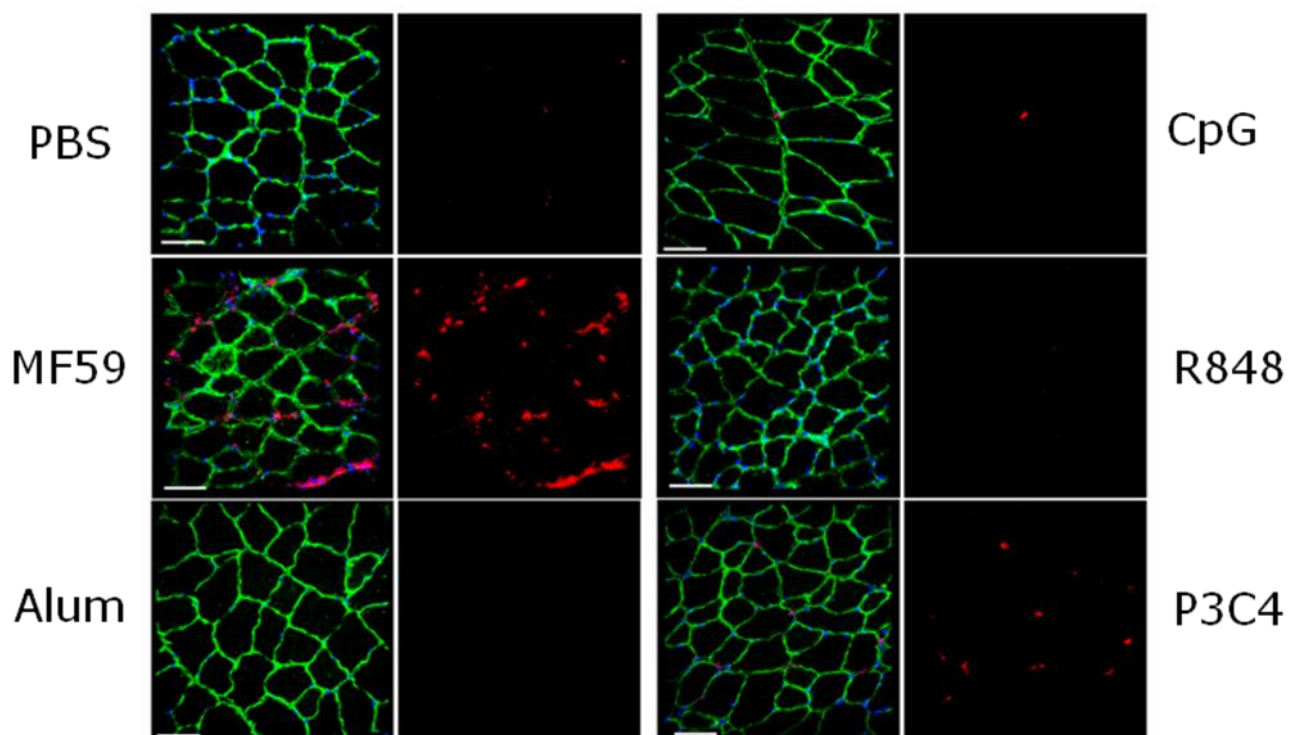


Figure 17: Confocal analysis of muscle cryosections at 6 h after treatment. Quadriceps were transversally sectioned at 5 μm fixed and stained with anti-utrophin antibody (green), anti-CD11b antibody (red) and a nuclear stain, ToPro3 (blue). Scale bar is 40 μm .

At 24 h MF59 still induced strong CD11b+ cell infiltration (fig. 18) and Pam3CSK4 led to strong infiltration of CD11b+ cells, but also induced some changes in muscle morphology.

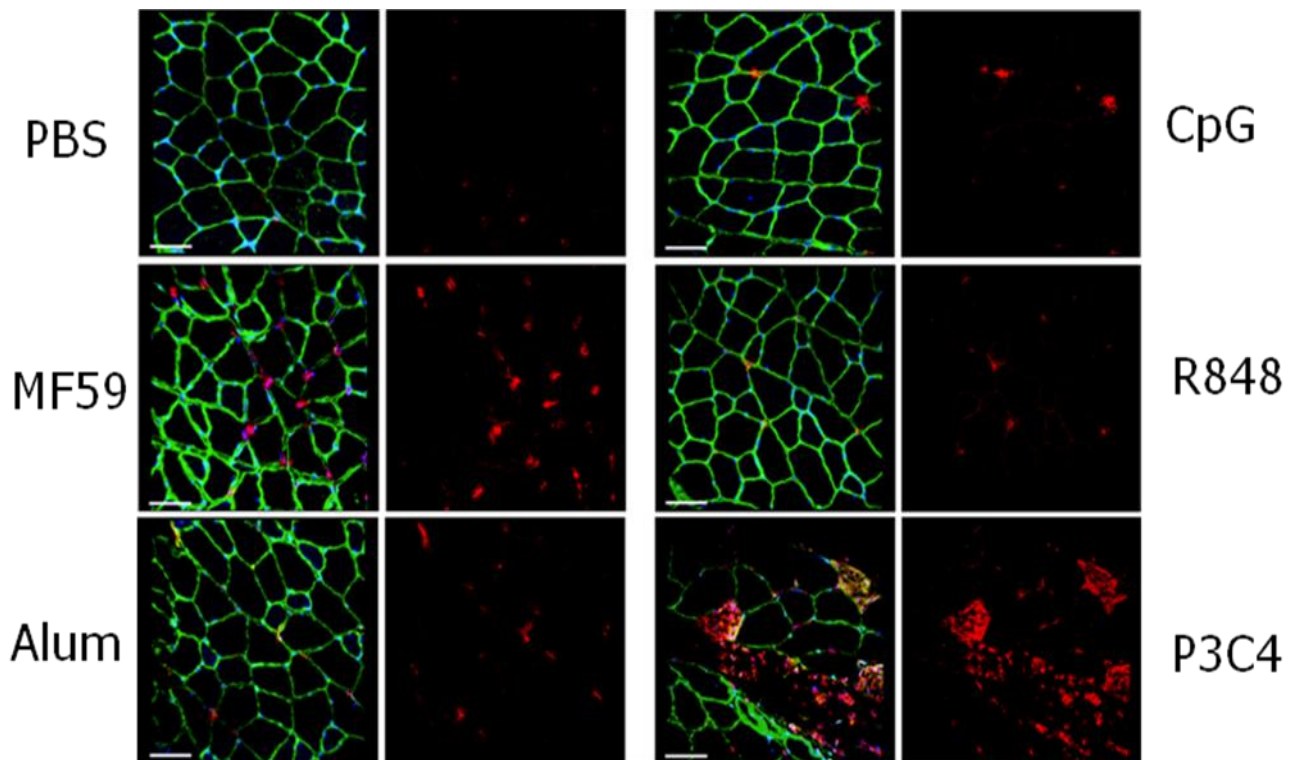


Figure 18: Confocal analysis of muscle cryosections at 24 h after treatment. Quadriceps were transversally sectioned at 5 μm fixed and stained with anti-utrophin antibody (green), anti-CD11b antibody (red) and a nuclear stain, ToPro3 (blue). Scale bar is 40 μm .

At the later time point, 4 days after treatment, the effect of Pam3CSK4 was even more dramatic, inducing strong CD11b+ cell infiltration and significant muscle destruction, suggesting that, at doses which are efficient for adjuvanticity, this compound was not as safe as MF59. Moreover at 4 days also CpG induced CD11b+ cell recruitment at injection site (fig.19).

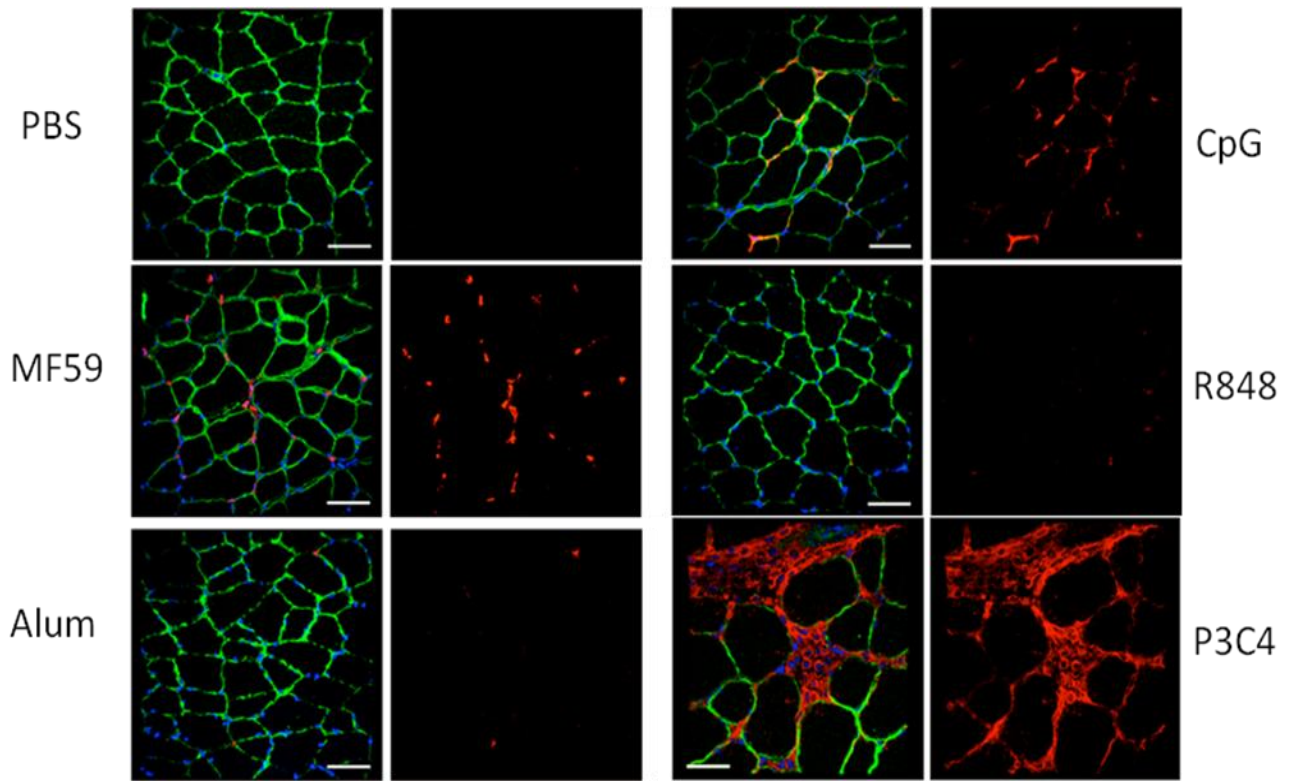


Figure 19: Confocal analysis of muscle cryosections at 4 days after treatment. Quadriceps were transversally sectioned at 5 μm fixed and stained with anti-utrophin antibody (green), anti-CD11b antibody (red) and a nuclear stain, ToPro3 (blue). Scale bar is 40 μm .

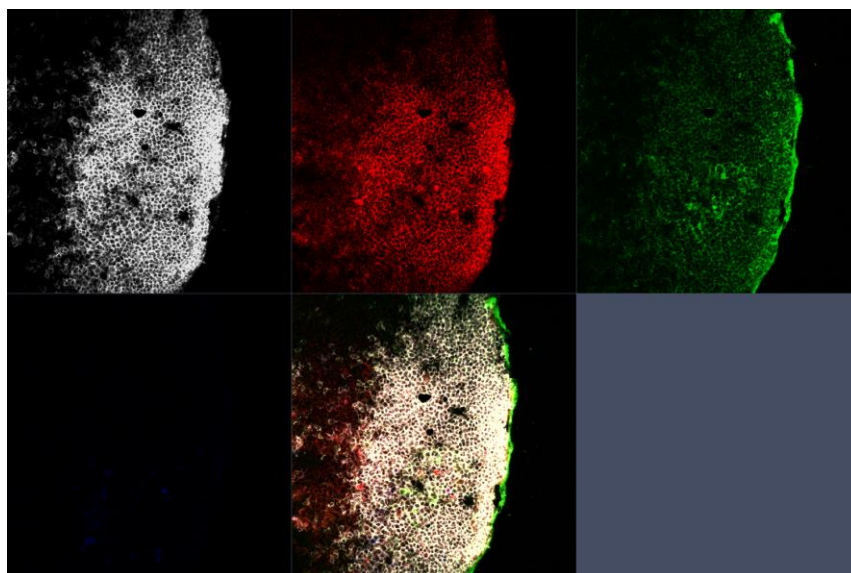
3.5 MF59 and Pam3CSK4 activate GL7 expression in the Germinal Centers of the lymph node.

Finally, in order to investigate if there was a differential activation of the LNs Germinal Centers induced by different adjuvants, we analyzed germinal centers formation in the lymph nodes. Germinal centers (GC) are the lymph node site where B cells undergo proliferation and selection and their formation is crucial for optimal high affinity antibody responses.

We investigated GC formation after treatment with flu + MF59 or flu + Pam3CSK4, the two adjuvants that induced significant Ab responses in adjuvanticity experiments (fig 1-4), flu alone and PBS as control.

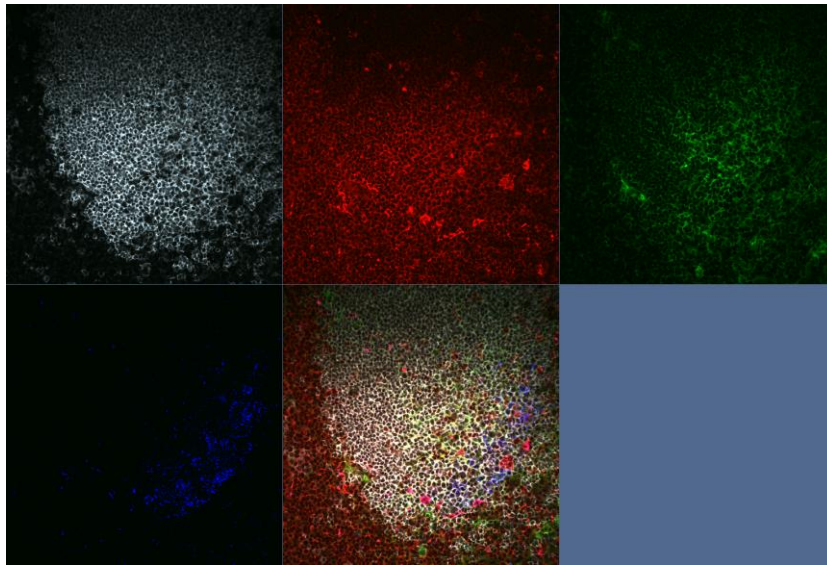
We analyzed LNs by immunofluorescence 2 weeks post second immunization. LNs cryosections were stained with anti-CD45R (B220) a marker specific for B cell areas, anti-CD3 that reveals T cell areas, anti-IgG and anti-GL7, that is a marker of Germinal Centers activation.

PBS



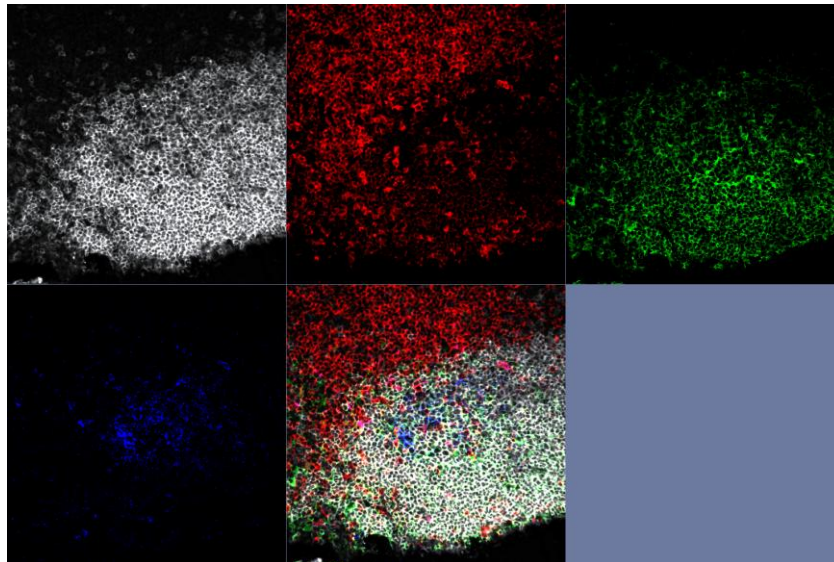
A

Flu



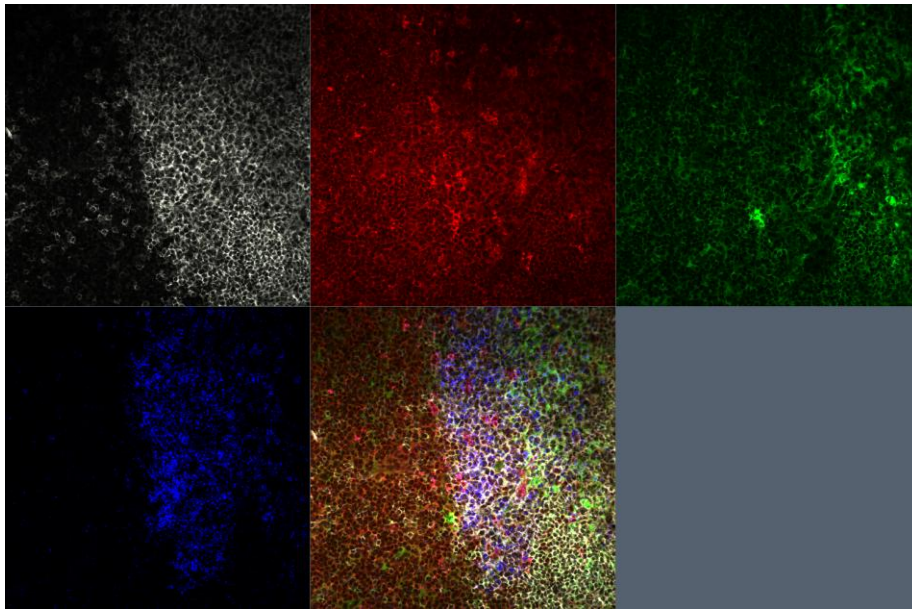
B

Flu + MF59



C

Flu + Pam3CSK4



D

Figure 19: Confocal analysis of lymph nodes cryosections 2 weeks post second immunization. Mice were injected with PBS (A), flu antigens (B), flu antigens plus MF59 (C) or flu antigens plus Pam3CSK4 (D). Tissue, stored in liquid nitrogen, was dissected, fixed and stained with anti-CD45R (white), anti-CD3 (red), anti IgG (green) and anti-GL7 (blue).

We observed an upregulation of GL7 expression in B cell areas of the LNs treated with flu antigens in combination with MF59 (fig. 19C) or Pam3CSK4 (fig.19D). Some GC activation was also observed after injection of flu antigens alone (fig 19B), in agreement with the lower immunogenicity of the flu antigens administered alone compared to flu + adjuvants.

4. Discussion of results and overview

There are different types of influenza virus vaccines: live attenuated influenza virus (LAIV), formalin-inactivated whole virus (WV) and “subunit” virus vaccine (SU) [59]. As mentioned before for this last type of vaccine Bernstein et al, in a paper published in 2008, demonstrated that a subvirion influenza A/H5N1 vaccine is more efficiently adjuvanted by the oil-in-water emulsion MF59 than alum [39]. Aluminum-containing adjuvants, the only adjuvants approved for human use in the United States, have been used routinely in a number of vaccines and have been investigated in conjunction with inactivated influenza vaccines. For seasonal influenza vaccines, aluminum hydroxide has not been shown to clearly increase immunogenicity. MF59 has been approved for use with seasonal influenza vaccines in several countries in Europe since 1997 and has been shown to improve antibody responses to influenza, herpes simplex, cytomegalovirus and HIV vaccines [37]. Although oil-in-water emulsions are considered promising candidates for several new human vaccines, their mode of action is still unclear.

Our main goal was to try to understand why MF59 induce better response to subunit flu vaccines, if compared to alum, and also the mechanism of action of flu adjuvanticity. In the current work we studied MF59 and alum, that are TLR-independent adjuvants, in comparison with three TLR-dependent adjuvants, CpG, R848 and Pam3CSK4.

We initially tested, in a mouse model, the activity of our set of vaccine adjuvants in combination with three different antigens: seasonal flu, tetanus toxoid and ovalbumin. Analyzing the antibody titers we observed that this adjuvanticity depends on the antigen. Strong flu specific total IgG titers induced by antigen co-administration with MF59 reflected clinical data, showing that MF59 induced a significant response to the trivalent flu antigens. Strong total IgG titers were also obtained with the TLR2 agonist Pam3CSK4, although to a lower extent. A strong adjuvant effect of both MF59 and Pam3CSK4 was also observed when these two adjuvants were administered together with OVA and TT antigens. Alum and CpG, even though they were not able to enhance total IgG titers to flu, could enhance immunogenicity of both OVA and TT antigens. R848, on the other hand, was the poorest adjuvant tested in our experiments, as it could only induce antibody titers to OVA.

These results are in line with previously published results and clearly demonstrate that adjuvanticity is strongly dependent on the antigen used in immunogenicity studies.

Analysis of antibody subclasses showed that MF59 induced significant IgG1 titers to all three antigen systems, confirming the fact that it is an inducer of Th2-biased responses in BALB/c mice [46-47]. Pam3CSK4 also was able to induce a mixed immune response, even though somehow Th2 biased, probably reflecting the species tested. On the other hand, as expected, the other TLR agonists, CpG and R848, gave stronger Th1 response, while alum induced a more Th2 biased antibody profile.

It is clear that the innate immune system plays a key role in determining the strength and quality of the adaptive immune response. For this reason, in order to understand if these differences in the adaptive response to flu correlated with innate immune reactions specific for each adjuvant, we analyzed the transcriptional profiles of these compounds at an early time point. We analyzed the whole mouse transcriptome *in vitro* 6 h after stimulation of mouse splenocytes, and *in vivo* in the mouse muscle and draining lymph nodes, 6 h after treatment.

One of the clusters of genes on which we focused our attention was the cytokine and chemokine genes cluster: in the following table we showed the number of regulated genes in the cluster for each treatment.

	spleno	muscle	LNs
MF59	0	36	0
Alum	0	11	0
CpG	24	18	0
R848	24	5	34
Pam3	20	8	12
Tot No. of genes selected	35	43	36

Tab. 4.1 Number of significantly regulated cytokines by tested adjuvants

As expected, the data clearly showed that the splenocytes were directly activated by TLRs, while the TLR-independent adjuvants did not activate cytokine gene expression in these cells. This was confirmed by the analysis of concentration of cytokines secreted by mouse splenocytes 6 h after stimulation with the compounds: IL-6, IL-10, IFN γ , TNF α , IL-12-p70 and KC were produced after CpG, R848 and Pam3CSK4 stimulation only.

On the contrary, at the injection site, we found that MF59 was the strongest inducer of cytokine genes, activating 36 over 43 selected cytokine genes. Another correlated cluster of genes, including genes encoding for transendothelial migration proteins, was also significantly activated by MF59 at the injection site and partially by CpG. Through the analysis of muscle cryosections 6 h after treatment with the various adjuvants, we monitored the recruitment of CD11b $^{+}$ cells into the muscle after adjuvant injection. In agreement with activation of genes involved in the recruitment of leukocytes, MF59 induced a significant infiltration of CD11b $^{+}$ cells compared to the control. These results were in agreement with results published by Mosca et al. JI, 2008 [33], and suggested that establishment of a local immunocompetent environment and a nonpathogenic inflammatory process is generally associated to vaccine adjuvanticity. A modest CD11b $^{+}$ cells recruitment at early time points was observed also after Pam3CSK4 injection. CD11b $^{+}$ cell recruitment positively correlated with enhanced total antibody titers to flu. Analyzing the kinetics of recruitment, we observed that MF59 was still able to recruit blood cells at the injection up to 4 days. Pam3CSK4 induced massive infiltration, which however resulted in muscle destruction. And CpG began to induce a significant recruitment of these cells only after 4 days in agreement with microarray data. These data suggested that mild and very early CD11b cell infiltration at injection site correlated to good adjuvanticity to flu antigens (MF59), without inducing reactogenicity (Pam3CSK4).

Compared to the muscle, we observed a completely different expression profile pattern in the draining lymph nodes. The TLR7/8 agonist R848 was the strongest activator of cytokine and chemokine genes. The same can be observed analyzing the cluster of IFN-related genes: R848 was the only activator of these genes in the LNs. It is likely that the strong activation of these genes reflects the pharmaco-kinetics/pharmaco-dynamics (PK/PD) properties of R848. This molecule is quickly released from the muscle to the circulation after injection and it is likely to immediately reach the LNs. R848 and CpG strongly regulated IFN genes also in the muscle and *in vitro* in mouse splenocytes (tab 4.2). Type I IFN are proteins endowed in multiple

biological activities and their production is markedly enhanced during infection [60]. More interestingly, in a recent published paper Koyama et al. demonstrated that WV influenza vaccines require TLR7-mediated IFN type I response for immunogenicity. Our results showed that strong activation of the interferon pathway in the muscle and in the LNs by the TLR7 adjuvant R848 was not sufficient to enhance the adaptive response to seasonal flu antigens.

	spleno	muscle	LNs
MF59	0	20	0
Alum	0	7	1
CpG	53	31	0
R848	55	36	61
Pam3	24	8	2
Tot No. of genes selected	64	60	62

Tab.4.2 Number of significantly regulated IFN genes by tested adjuvants.

By multicolor FACS staining we confirmed that activation of lymph node cells occurred only after treatment with R848, and not with the other adjuvants. We observed an up-regulation of CD69 in T, B and NK cells, an up-regulation of CD86 in B cells and an increased number of DCs that express high level of CD86 and MHC class II molecules. These results were consistent with microarray data.

To address whether adjuvanticity to flu antigens is correlated to increased antigen uptake from antigen presenting cells or a more efficient APCs migration to the lymph nodes, we performed flow cytometric analysis of LNs single cell suspensions after i.m. injection with fluorescent antigen alone or in combination with the various adjuvants. 24 h after i.m. injection of 10 µg of the Alexa Fluor488-labeled H1N1 A/Brisbane 2007 antigen (present in the trivalent seasonal flu formulation used in the previous experiments) alone or in combination with the adjuvants used in this study, we did not detect the presence of any antigen-positive cell in the LNs. The same analysis performed at earlier time points (1 h, 3 h and 6 h) using MF59-treated mice revealed that the addition of MF59 did not increase the

number of antigen positive DCs (CD11c+ cells), monocytes (Ly6C+) or B cells (fig.16). These data suggest that MF59 did not increase the number of antigen-positive APCs in the LNs. However, it might also be possible that we were unable to detect those cells because of degradation of the antigen or because the number of the antigen-positive cells is under the detection limit.

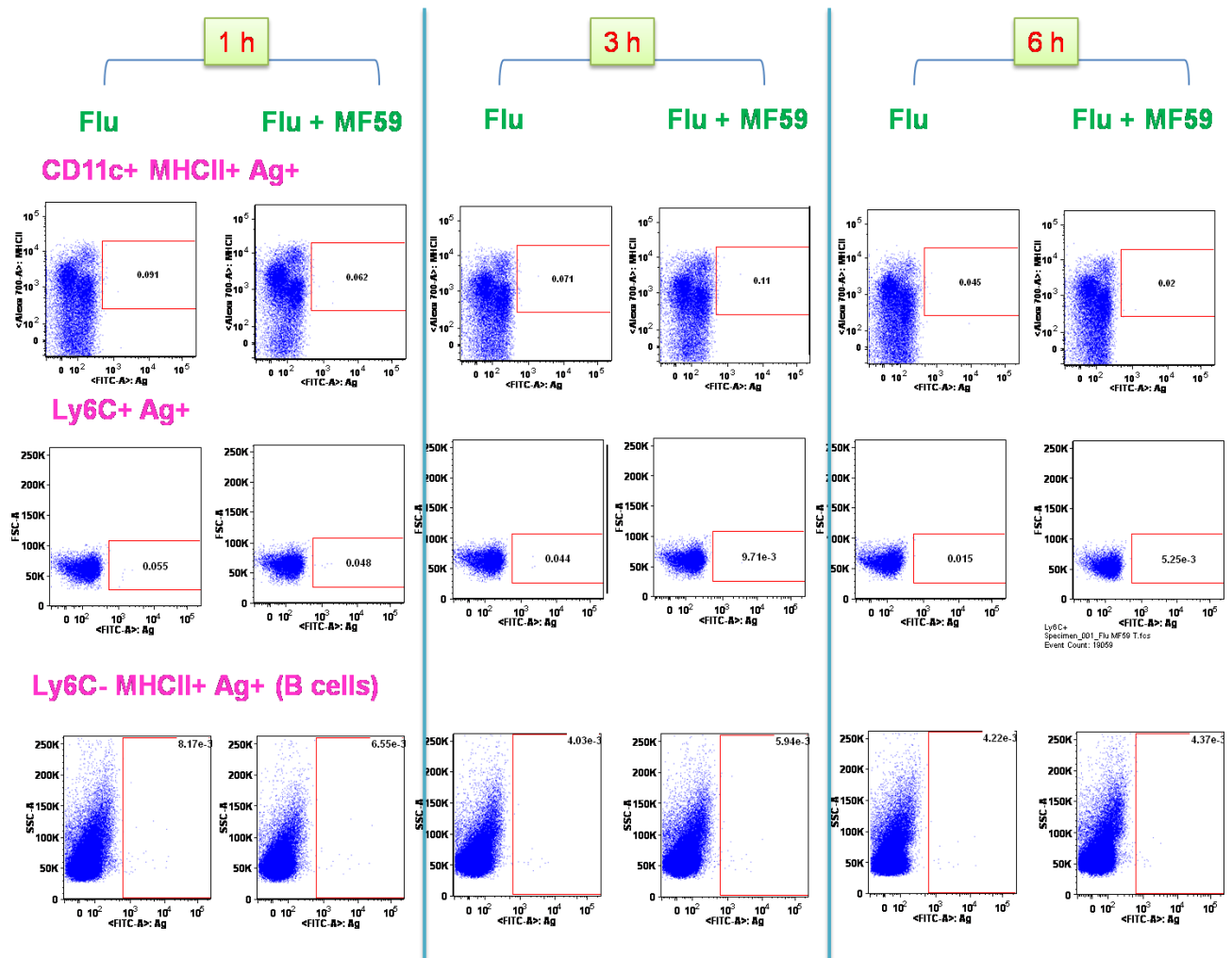


Figure 20: Multi-color flow cytometric analysis of antigen-positive cells isolated from the draining LNs 1 h, 3 h and 6 h after i.m. injection with H1N1-AlexaFluor488 labeled alone or in combination with MF59. After SSC vs. FSC gating on live cells to isolate lymphocytes, and SSC vs. SSW gating to isolate single events, DCs cells were identified as CD11c+/MHCII+ cells, monocytes as Ly6C+ cells and B cells as Ly6C-/MHCII+ cells.

Finally we wanted to investigate the formation of Germinal Centers (GCs) in the lymph nodes induced by different adjuvants 2 weeks post second immunization focusing our attention on flu + MF59-treated mice and flu + Pam3CSK4-treated mice. GCs are a source of effector B cell populations and are crucial for the generation of humoral immunity: in particular the function of GCs is to generate the high affinity antibodies that form a key defense against infectious pathogens and are crucial to the efficacy of virtually all vaccines [61]. Performing immunofluorescence analysis of LNs cryosections, we noted an up-regulation of GL7 (a biomarker of GCs activation) expression in the B cell area of LNs treated with flu in combination with MF59 and with Pam3CSK4. These findings strongly correlated with the fact that these were the two adjuvants that induced significant antibody titers to flu in the adjuvanticity experiments. In order to establish a strong correlation between GCs formation in the LNs and antibodies production we would need to further analyze this aspect, by performing both a kinetic analysis in order to find the peak of GC activation and by assessing the effects of the other adjuvants in relation to the same readout.

In summary, here we show that strong activation of innate immunity in the muscle, but not in draining LNs, and local recruitment of CD11b⁺ blood cells at injection site by MF59 and TLR2 vaccine adjuvants strongly correlate with the ability of these adjuvants to enhance antibody responses to flu antigens. Moreover, we found that the TLR7 adjuvant R848 did not affect the adaptive response to flu despite a strong activation of the interferon pathway in the muscle and in the LNs. To better understand whether the adjuvanticity of R848 is dependent on a functional type I IFN pathway, we will perform in the near future a comparative adjuvanticity experiment in which mice have been previously injected with type I IFN receptor blocking antibody or isotype control. We expect that the molecules that depend on a functional IFN type I pathway will not be able to enhance antigen-specific antibody titers in animals that have a blocked IFN type I pathway, while the IFN-independent adjuvants (MF59) will still be able to give enhanced antibody responses to these model antigens.

5. References

- [1] Glenny AT, Pope CG, Waddington H, Wallace U. Immunological notes XVII to XXIV. J Pathol 1926;29:31–40.
- [2] Ramon, G. (1926) Procéde's pour accroître la production des antitoxines. Ann. Inst. Pasteur 40, 1–10.
- [3] Akira S, Uematsu S, Takeuchi O: Pathogen recognition and innate immunity. Cell 2006, 124:783-801.
- [4] Janeway CA Jr, Medzhitov R: Innate immune recognition. Annu Rev Immunol 2002, 20:197-216.
- [5] Brunner R, Jensen-Jarolim E, Pali-Schöll I, The ABC of clinical and experimental adjuvants—A brief overview. Immunology Letters 128 (2010) 29–35
- [6] J. Ishii K , and Akira S: Toll or Toll-Free Adjuvant Path Toward the Optimal Vaccine Development . Journal of Clinical Immunology, Vol. 27, No. 4, 2007
- [7] Guy B: The perfect mix: recent progress in adjuvant research. Nat Rev Microbiol 2007, 5:505-517.
- [8] Garçon N, Chomez P, Van Mechelen M: GlaxoSmithKline adjuvant systems in vaccines: concepts, achievements and perspectives. Expert Rev Vaccines 2007, 6:723-739.
- [9] Lambrecht B N, Kool M, Willart M AM and Hammad H: Mechanism of action of clinically approved adjuvants. Current Opinion in Immunology 2009, 21:1–7
- [10] Gupta RK, Rost BE, Relyveld E, Siber GR. Adjuvant properties of aluminum and calcium compounds. Pharm Biotechnol 1995;6:229–48.
- [11] Brewer JM: (How) do aluminium adjuvants work? Immunol Lett 2006, 102:10-15.
- [12] HogenEsch H: Mechanisms of stimulation of the immune response by aluminum adjuvants. Vaccine 2002, 20(Suppl3):S34-39.
- [13] Hem SL, Hogenesch H: Relationship between physical and chemical properties of aluminum-containing adjuvants and immunopotential. Expert Rev Vaccines 2007, 6:685-698.
- [14] Morefield GL, Sokolovska A, Jiang D, HogenEsch H, Robinson JP, Hem SL: Role of aluminum-containing adjuvants in antigen internalization by dendritic cells in vitro. Vaccine 2005, 23:1588-1595.

- [15] Kool M, Soullie T, van Nimwegen M, Willart MA, Muskens F, Jung S, Hoogsteden HC, Hammad H, Lambrecht BN: Alum adjuvant boosts adaptive immunity by inducing uric acid and activating inflammatory dendritic cells. *J Exp Med* 2008, 205:869-882.
- [16] Wack, A., Baudner, B. C., Hilbert, A. K., Manini, I., Nuti, S., Tavarini, S., Scheffczik, H. et al., Combination adjuvants for the induction of potent, long-lasting antibody and T-cell responses to influenza vaccine in mice. *Vaccine* 2008. 26: 552–561.
- [17] Gavin AL, Hoebe K, Duong B, Ota T, Martin C, Beutler B, Nemazee D: Adjuvant-enhanced antibody responses in the absence of toll-like receptor signaling. *Science* 2006, 314:1936-1938.
- [18] Petrilli V, Dostert C, Muruve DA, Tschopp J: The inflammasome: a danger sensing complex triggering innate immunity. *Curr Opin Immunol* 2007, 19:615-622.
- [19] Fritz JH, Ferrero RL, Philpott DJ, Girardin SE: Nod-like proteins in immunity, inflammation and disease. *Nat Immunol* 2006, 7:1250-1257.
- [20] Li H, Nookala S, Re F: Aluminum hydroxide adjuvants activate caspase-1 and induce IL-1beta and IL-18 release. *J Immunol* 2007, 178:5271-5276.
- [21] Eisenbarth SC, Colegio OR, O'Connor W, Sutterwala FS, Flavell RA: Crucial role for the Nalp3 inflammasome in the immunostimulatory properties of aluminium adjuvants. *Nature* 2008, 453:1122-1126.
- [22] Kool M, Petrilli V, De Smedt T, Rolaz A, Hammad H, van Nimwegen M, Bergen IM, Castillo R, Lambrecht BN, Tschopp J: Cutting edge: alum adjuvant stimulates inflammatory dendritic cells through activation of the NALP3 inflammasome. *J Immunol* 2008, 181:3755-3759.
- [23] Li H, Willingham SB, Ting JP, Re F: Cutting edge: inflammasome activation by alum and alum's adjuvant effect are mediated by NLRP3. *J Immunol* 2008, 181:17-21.
- [24] Franchi L, Nunez G: The Nlrp3 inflammasome is critical for aluminium hydroxide-mediated IL-1beta secretion but dispensable for adjuvant activity. *Eur J Immunol* 2008, 38:2085-2089.
- [25] Kool M, Soullie T, van Nimwegen M, Willart MA, Muskens F, Jung S, Hoogsteden HC, Hammad H, Lambrecht BN: Alum adjuvant boosts adaptive immunity by inducing uric acid and activating inflammatory dendritic cells. *J Exp Med* 2008, 205:869-882.
- [26] Becker BF: Towards the physiological function of uric acid. *Free Radic Biol Med* 1993, 14:615-631.

- [27] Hassoun PM, Yu FS, Cote CG, Zulueta JJ, Sawhney R, Skinner KA, Skinner HB, Parks DA, Lanzillo JJ: Upregulation of xanthine oxidase by lipopolysaccharide, interleukin-1, and hypoxia. Role in acute lung injury. *Am J Respir Crit Care Med* 1998, 158:299-305.
- [28] De Gregorio E, Tritto E, Rappuoli R: Alum adjuvanticity: unraveling a century old mystery. *Eur. J. Immunol.* 2008. 38: 2068-2071.
- [29] Schultze V, D'Agosto V, Wack A, Novicki D, Zorn J, Hennig R. Safety of MF59 adjuvant. *Vaccine* 2008;26 (June (19):3209.
- [30] Cataldo, D.M. and Van Nest, G. (1997) The adjuvant MF59 increases the immunogenicity and protective efficacy of subunit influenza vaccine in mice. *Vaccine* 15, 1710–1715.
- [31] Dupuis M, Denis-Mize1 K, LaBarbara A, Peters W, Charo IF, McDonald DM, et al. Immunization with the adjuvant MF59 induces macrophage trafficking and apoptosis. *Eur J Immunol* 2001;31:2910–8.
- [32] Dupuis M, Murphy TJ, Higgins D, Ugozzoli M, Van Nest G, Ott G, et al. Dendritic cells internalize vaccine adjuvant after intramuscular injection. *Cell Immunol* 1998;186:18–27.
- [33] Mosca F, Tritto E, Muzzi A, Monaci E, Bagnoli F, Iavarone C, O'Hagan D, Rappuoli R, De Gregorio E: Molecular and cellular signatures of human vaccine adjuvants. *Proc Natl Acad Sci U S A* 2008, 105:10501-10506.
- [34] Wack A, Baudner BC, Hilbert AK, Manini I, Nuti S, Tavarini S, Scheffczik H, Ugozzoli M, Singh M, Kazzaz J et al.: Combination adjuvants for the induction of potent, long-lasting antibody and T-cell responses to influenza vaccine in mice. *Vaccine* 2008, 26:552-561.
- [35] Klinman DM, Currie D, Gursel I, Verthelyi D. Use of CpG oligodeoxynucleotides as immune adjuvants. *Immunol Rev* 2004;199:201—16.
- [36] Ott G, Radhakrishnan R, Fang J-H, Hora M. The adjuvant MF59: a ten year perspective. In: O'Hagan D, editor. *Vaccine adjuvants: preparation methods and research protocols*. Totowa, NJ: Humana Press; 2001. p. 211—28.
- [37] Podda A, Del Giudice G. MF59-adjuvanted vaccines: increased immunogenicity with an optimal safety profile. *Expert Rev Vaccines* 2003;2(2):197—203.
- [38] Podda A, Del Giudice G. MF59 adjuvant emulsion. In: Levine MM, Kaper JB, Rappuoli R, Liu MA, Good MF, editors. *New generations vaccines*. 3rd edition New York: Marcel Dekker; 2004. p. 225–36.

- [39] Bernstein D I, Edwards K M, Dekker C L, Belshe R, Talbot H K B, Graham I L, Noah D L, He F, and Hill H: Effects of Adjuvants on the Safety and Immunogenicity of an Avian Influenza H5N1 Vaccine in Adults. *JID* 2008:197
- [40] Nicholson KG, Colegate AE, Podda A, et al. Safety and antigenicity of non-adjuvanted and MF59-adjuvanted influenza A/Duck/Singapore/97 (H5N3) vaccine: a randomised trial of two potential vaccines against H5N1 influenza. *Lancet* 2001; 357:1937– 43.
- [41] Atmar RL, Keitel WA, Patel SM, et al. Safety and immunogenicity of non-adjuvanted and MF59-adjuvanted influenza A/H9N2 vaccine preparations. *Clin Infect Dis* 2006; 43:1135– 42.
- [42] Frey S, Poland G, Percell S and Podda A. Comparison of the safety, tolerability, and immunogenicity of a MF59-adjuvanted influenza vaccine and a non-adjuvanted influenza vaccine in non-elderly adults. *Vaccine* 2003; 21:4234 –7.
- [43] Minutello M, Senatore F, Cecchinelli G, et al. Safety and immunogenicity of an inactivated subunit influenza virus vaccine combined with MF59 adjuvant emulsion in elderly subjects, immunized for three consecutive influenza seasons. *Vaccine* 1999; 17:99 –104.
- [44] Janeway's Immunobiology seventh edition. Murphy K, Travers P, Walport M. 2008.
- [45] Chiarella P, Massi E, De Robertis M, Signori E, Fazio V M. Adjuvants in vaccines and for immunisation: current trends. *Expert Opin. Biol. Ther.* 2007; 7(10):1551-1562.
- [46] Valensi J P, Carlson J R, and Van Nest G A. Systemic Cytokine Profiles in BALB/c Mice immunized with trivalent influenza vaccine containing MF59 oil emulsion and other advanced adjuvants. *The Journal of Immunology*, 1994, 153: 4029.
- [47] Baudner B C, Ronconi V, Casini D, Tortoli M, Kazzaz J, Singh M, Hawkins L D, Wack A and O'Hagan D T. MF59 Emulsion Is an Effective Delivery System for a Synthetic TLR4 Agonist (E6020). *Pharmaceutical Research*, Vol. 26, No. 6, June 2009.
- [48] Guiducci C, Coffman R L, Barrat F J. Signalling pathways leading to IFN- α production in human plasmacytoid dendritic cell and the possible use of agonists or antagonists of TLR7 and TLR9 in clinical indications. *Journal of Internal Medicine* 265; 43–57. 2008.
- [49] Kadowaki N and Liu Y. Natural Type I Interferon-Producing Cells as a link between innate and adaptive immunity. *Human Immunology* 63, 1126–1132 (2002)
- [50] Gorden K B, Gorski K S, Gibson S J, et al.. Synthetic TLR agonists reveal functional differences between human TLR7 and TLR8. *J. Immunol.* 174(3), 1259-1268 (2005).

- [51] Hemmi H, Kaisho T, Takeuchi O, *et al.* Small anti-viral compounds activate immune cells via the TLR7 MyoD88-dependent signaling pathway. *Nat. Immunol.* 3(2), 196-200 (2002).
- [52] Tomai M A, Miller R L, Kenneth E L, Kieper W C, Zarraga I E, Vasilakos J P. Resiquimod and other immune response modifiers vaccine adjuvants. *Expert Rev. Vaccines* 6(5), 835-847 (2007).
- [53] Black M, Trent A, Tirrell M and Olive C. Advances in the design and delivery of peptide subunit vaccines with a focus on Toll-like receptor agonists. *Expert Rev. Vaccines* 9(2), 157–173 (2010).
- [54] Takeuchi O, Hoshino K, Kawai T, Sanjo H, Takada H, Ogawa T, Takeda K, Akira S, *Immunity* 11 (1999) 443-451.
- [55] Takeuchi O, Kaufmann A, Grote K, Kawai T, Hoshino K, Morr M, Muhlradt P F, Akira S, *J. Immunol.* 164 (2000). 554-557.
- [56] A. Ozinsky, D.M. Underhill, J.D. Fontenot, A.M. Hajjar, K.D. Smith, C.B. Wilson, L. Schroeder, A. Aderem, *Proc. Natl. Acad. Sci. USA* 97 (2000) 13766-13771.
- [57] Antonios O. Aliprantis, *et al.* Cell Activation and Apoptosis by Bacterial Lipoproteins Through Toll-like Receptor-2. *Science* 285, 736 (1999).
- [58] McKee A M, Munks M W, MacLeod K L M, Fleenor C J, Van Rooijen N, Kappler J W and Marrack P. Alum induces innate immune responses through macrophage and mast cell sensors, but these sensors are not required for alum to act as an adjuvant for specific immunity. *J. Immunol.* 2009;183;4403-4414. 2009.
- [59] Koyama S, Aoshi T, Tanimoto T, Kumagai Y, Kobijama K, Tougan T, Sakurai K, Coban C, Horii T, Akira S, Ishii K J. Plasmacitoid dendritic cells delineate immunogenicity of influenza vaccine subtypes. *Sci. Transl. Med.* 2, 25ra24 (2010).
- [60] Proietti E, Bracci L, Puzelli S, Di Pucchio T, Sestili P, De Vincenzi E, Venditti M, Capone I, Seif I, De Maeyer E, Tough D, Donatelli I, Belardelli F. Type I IFN is a natural adjuvant for protective immune response: lessons from the influenza vaccine model. *J. Immunol.* 169;375-383. 2002.
- [61] Gatto D and Brink R. The germinal center reaction. *J Allergy Clin Immunol.* 126:898-907. 2010.

Acknowledgements

Thanks to:

Dott. Ennio De Gregorio (Novartis Vaccines & Diagnostics, Siena)

Dott.ssa Elaine Tritto (Novartis Vaccines & Diagnostics, Siena)

Prof. Cesare Montecucco (University of Padova)